Behavioral/Systems/Cognitive

HDAC6 Regulates Glucocorticoid Receptor Signaling in Serotonin Pathways with Critical Impact on Stress Resilience

Julie Espallergues,[1]* Sarah L. Teegarden,[1]* Avin Veerakumar,[1] Janette Boulden,[1] Collin Challis,[1] Jeanine Jochems,[1] Michael Chan,[1] Tess Petersen,[1] Evan Deneris,[3] Patrick Matthias,[4] Chang-Gyu Hahn,[1] Irwin Lucki,[1] Sheryl G. Beck,[2] and Olivier Berton[1]

[1]Department of Psychiatry, University of Pennsylvania Medical School, and [2]Department of Anesthesiology, Children's Hospital of Philadelphia Research Institute and University of Pennsylvania, Philadelphia, Pennsylvania 19104, [3]Department of Neuroscience, School of Medicine, Case Western Reserve University, Cleveland, Ohio 44106, and [4]Friedrich Miescher Institute for Biomedical Research, CH-4058 Basel, Switzerland

Genetic variations in certain components of the glucocorticoid receptor (GR) chaperone complex have been associated with the development of stress-related affective disorders and individual variability in therapeutic responses to antidepressants. Mechanisms that link GR chaperoning and stress susceptibility are not well understood. Here, we show that the effects of glucocorticoid hormones on socioaffective behaviors are critically regulated via reversible acetylation of Hsp90, a key component of the GR chaperone complex. We provide pharmacological and genetic evidence indicating that the cytoplasmic lysine deacetylase HDAC6 controls Hsp90 acetylation in the brain, and thereby modulates Hsp90 –GR protein–protein interactions, as well as hormone- and stress-induced GR translocation, with a critical impact on GR downstream signaling and behavior. Pet1-Cre-driven deletion of HDAC6 in serotonin neurons, the densest HDAC6-expressing cell group in the mouse brain, dramatically reduced acute anxiogenic effects of the glucocorticoid hormone corticosterone in the open-field, elevated plus maze, and social interaction tests. Serotonin-selective depletion of HDAC6 also blocked the expression of social avoidance in mice exposed to chronic social defeat and concurrently prevented the electrophysiological and morphological changes induced, in serotonin neurons, by this murine model of traumatic stress. Together, these results identify HDAC6 inhibition as a potential new strategy for proresilience and antidepressant interventions through regulation of the Hsp90 –GR heterocomplex and focal prevention of GR signaling in serotonin pathways. Our data thus uncover an alternate mechanism by which pan-HDAC inhibitors may regulate stress-related behaviors independently of their action on histones.

Introduction

A proportion of patients who experience interpersonal violence subsequently develop psychiatric conditions, such as posttraumatic stress disorder (PTSD) and mood disorders (Charuvastra and Cloitre, 2008). Likewise, in various animal species, assaults from conspecifics can elicit indelible changes in affective behaviors (Sapolsky, 2005; Huhman, 2006). We and others have shown that a majority of mice exposed to repeated bouts of severe aggression develop an enduring form of social avoidance that can be treated efficiently by chronic administration of antidepressant drugs (Kudryavtseva et al., 1991; Berton et al., 2006; Tsankova et al., 2006). In contrast, a small proportion of mice within each cohort exposed to chronic social defeat consistently fail to develop these behavioral abnormalities. We have taken advantage of this dichotomy in earlier studies to identify molecular signatures that discriminate vulnerable mice from their resilient and antidepressant-treated counterparts (Berton et al., 2006; Krishnan et al., 2007). These studies have identified histone deacetylases (HDACs) as a class of molecular modulators of resilience and antidepressant responses (Tsankova et al., 2006; Renthal et al., 2007). HDACs comprise a family of lysine deacetylases that regulate protein functions by removing acetyl groups from lysine side chains. Broad pharmacological inhibition of class I and/or class II HDACs has recently been shown to normalize social defeat-induced behavioral deficits (Covington et al., 2009). The unavailability of true isoform-selective HDAC inhibitors (HDACis) (Bradner et al., 2010) has so far impeded the identification of the specific isoforms responsible for these antidepressant-like effects.

Although most studies on the roles of HDACs in the brain have been centered on the canonical function of these enzymes (Haggarty and Tsai, 2011), recent proteomics studies have revealed that histones represent only a fraction of the HDACi-regulated acetylome (Choudhary et al., 2009; Spange et al., 2009; Zhao et al., 2010). This suggests that a variety of unex-

Received Nov. 8, 2011; revised Jan. 10, 2012; accepted Feb. 5, 2012.

Author contributions: J.E., S.L.T., and O.B. designed research; J.E., S.L.T., A.V., J.B., C.C., J.J., M.C., T.P., I.L., and S.G.B. performed research; E.D., P.M., and C.-G.H. contributed unpublished reagents/analytic tools; J.E., S.L.T., A.V., J.B., M.C., T.P., C.-G.H., I.L., S.G.B., and O.B. analyzed data; J.E., S.L.T., S.G.B., and O.B. wrote the paper.

This work was supported by National Institute of Mental Health (NIMH) Grants MH087581 (O.B.) and MH0754047 (S.G.B.), and grants from the International Mental Health Research Organization (O.B., C.-G.H.) and from the National Alliance for Research on Schizophrenia and Depression (O.B.), and by postdoctoral fellowships from the Fyssen Foundation (J.E.) and NIMH (S.L.T.). Many thanks to Marisa Johns for excellent technical assistance. We thank Drs. Stephen Haggarty and Ralph Mazitschek for the generous gift of tubacin, Dr. Tso-Pang Yao for providing the anti-mouse HDAC6 antibody, and Dr. E. Seto for mouse HDAC plasmids. We thank Dr. William Renthal for his comments on the manuscript.

The authors declare no competing financial interests.

*J.E. and S.L.T. contributed equally to this work.

Correspondence should be addressed to Olivier Berton at the above address. E-mail: bertonol@upenn.edu.

DOI:10.1523/JNEUROSCI.5634-11.2012

 0270-6474/12/324400-17$15.00/0

plored histone-independent mechanisms are likely to contribute to the psychopharmacological activity of these drugs.

HDAC6, a cytoplasmic class IIb isoform, is a prime candidate to mediate histone-independent effects of pan-HDAC inhibitors (Verdel et al., 2000; Hubbert et al., 2002). A well characterized class of substrates for HDAC6 comprises the proteins of the heat shock family, including Hsp90 (Aoyagi and Archer, 2005; Bali et al., 2005; Kovacs et al., 2005). Hyperacetylation of Hsp90 following HDAC6 depletion has been shown to alter the assembly of the glucocorticoid receptor (GR) chaperone complex and impair downstream cellular responses to glucocorticoid hormones (Kovacs et al., 2005; Murphy et al., 2005; Scroggins et al., 2007; Zhang et al., 2008). To date, this role of HDAC6 as regulator of GR responses has never been examined in the CNS. Because certain alterations in the dynamics of the Hsp90–GR heterocomplex have been directly implicated as vulnerability factors in PTSD and mood disorders (Binder et al., 2004; Maeng et al., 2008; Binder, 2009; Hunsberger et al., 2009), we hypothesized that HDAC6 may act as a critical upstream regulator of stress resilience. We tested this hypothesis by examining the effect of a loss of function of HDAC6 in murine models of stress-related affective disorders.

Materials and Methods

Animals

Eight- to 12-week-old male mice bred onto a C57BL/6 background were used for all experiments. Mice were housed on a 12 h light/dark cycle with food and water available *ad libitum*. All studies were conducted according to protocols approved by the University of Pennsylvania Institutional Animal Care and Use Committee, and all procedures were performed in accordance with institutional guidelines.

To generate a mouse line with a selective inactivation of the HDAC6 gene in serotonin neurons, male BAC transgenic Pet1-Cre mice (Scott et al., 2005) were crossed to flHDAC6 females in which a portion of HDAC6 gene (exons 8–10) is floxed (Zhang et al., 2008). Earlier experimental evidence indicated that Cre-induced recombination in flHDAC6 mice ablates a portion of the gene encoding the first catalytic domain of the enzyme, and produces a frameshift that leads to a complete loss of HDAC6 transcript and function (Zhang et al., 2008; Bobrowska et al., 2011). Pet1-Cre-driven KO (referred to as $HDAC6^{Pet1Cre}$) was used in all experiments reported here with the exception of protein measurements by Western blot with or without previous immunoprecipitation or nuclear extraction that required a higher amount of starting material and were conducted from gross brainstem dissections in pan-neuronal, Nestin-Cre driven HDAC6 KO mice (referred to as $HDAC6^{NestinCre}$). The latter line was bred by crossing males from B6.Cg-Tg(Nes-cre)1Kln/J line (JAX stock number 003771) with flHDAC6 females as described above.

Immunohistochemistry

Tissues were collected from animals transcardially perfused with 4% paraformaldehyde and sectioned on a freezing microtome at a thickness of 30 μm. A custom-made polyclonal antibody kindly provided by Dr. Tso-Pang Yao (Duke University, Durham, NC) was used for the detection of HDAC6. This antibody was raised in rabbits by injection of a GST-tagged C terminus fragment of mouse HDAC6 protein (amino acids 991–1149) and affinity purified (Gao et al., 2007). A dedicated stereological software (Stereo Investigator; MBF Bioscience) was used for unbiased sampling and stereological counting using an Optical Fractionator probe. For further characterization of the cell populations expressing HDAC6, double-label immunohistochemistry (IHC) was conducted using antibodies for cell type-specific markers followed by fluorescent secondary antibodies and analyzed using confocal microscopy. Antibodies for tryptophan hydroxylase (TPH) (AB1541), NeuN (AB377), and GFAP (AB360) were obtained from Millipore. GR antibody (H-300) was obtained from Santa Cruz Biotechnology. AcHsp90 antibody was obtained from Rockland Immunochemicals.

In situ *hybridization*

Studies were conducted as described previously (Berton et al., 2007). Briefly, brains were flash-frozen by immersion into isopentane at −25°C, and kept at −80°C until sectioned. An antisense probe was generated for HDAC6 (980 bp fragment corresponding to exons 17–24 of HDAC6). For *in vitro* transcription of HDAC6 antisense probes, vector was linearized and transcribed using SP6 RNA polymerase in the presence of ^{35}S-UTP and purified using the MEGAclear Kit (Ambion). Tissue was hybridized overnight at 55°C, washed, and exposed to autoradiographic film for up to 1 week.

Behavioral studies

Social defeat and social avoidance testing. Social defeat and social avoidance testing were conducted as previously reported (Berton et al., 2006; Golden et al., 2011). Male CD1 retired breeders, selected on the basis of their reliable expression of aggressive behaviors, were used to physically defeat the experimental mice for 5 min each day. Experimental mice were then housed for the remainder of the time in protected sensory contact with the CD1 aggressor through a Plexiglas partition. Defeats were repeated for 10 consecutive days with mice rotated each day into the cage of a new CD1 aggressor. Control animals were housed in similar partitioned cages with another mouse from the same genotype and handled daily. On day 11, social approach/avoidance behavior toward an unfamiliar social target was examined in a two-trial social interaction test. In the first 2.5 min trial ("target absent"), the experimental mice were allowed to freely explore a dimly lit (55 lux) open-field arena containing an empty wire mesh cage (10 × 6 cm) positioned on one side of the arena (see Fig. 5*c*). During the second 2.5 min trial ("target present"), experimental mice were reintroduced into the arena with the wire mesh cage now containing an unfamiliar CD1 aggressor mouse. Videotracking software (Topscan; CleverSys) was used to measure the time spent in the "interaction zone" (a 14 × 26 cm rectangle surrounding the target box). Interaction ratios (IRs) were calculated as the percentage time spent in interaction zone in the target-present relative to the target-absent condition. Vulnerable (IR $<$ 100) and resilient mice (IR $\geq$ 100) were determined as described previously (Krishnan et al., 2007; Golden et al., 2011).

Tail suspension test and forced-swim test. These procedures were conducted as previously reported (Crowley et al., 2004). Assessments were conducted using an automated device (MED Associates) in the tail suspension test (TST) or using TopScan videotracking software (CleverSys) for the forced-swim test (FST).

Behavioral effects of acute corticosterone. Mice were given a single injection of 0.5 mg/kg Cort-HBC (Sigma-Aldrich) intraperitoneally or saline vehicle 20 min before the initiation of the test. Social interaction (SI) tests were conducted exactly as described above. For the open-field (OF) test, mice were placed in the center of an open arena identical with that used for social interaction, but lacking the target box. The test lasted for 5 min and TopScan 2.0 software was used to determine the number of entries and time in the center area as well as the total distance traveled. Both SI and OF were conducted under 55 lux illumination. In the elevated plus maze (EPM), made of two perpendicular intersecting runways, each 7.6 cm wide and 60 cm long positioned on a pedestal 30 cm above the floor, the same videotracking system was used to measure the time spent and numbers of entries in open and closed arms. Illumination was 10 lux when measured in open arms of the EPM.

Raphe slice preparation for electrophysiological and morphological studies

Coronal raphe slices (200 μm thick) were prepared as previously reported (Beck et al., 2004) using a Leica microslicer (Leica) and placed in a holding vial containing ACSF with L-tryptophan (50 μM) at 35°C bubbled with 95% O_2/5% CO_2 for 1 h. Slices were then maintained in room temperature ACSF bubbled with 95% O_2/5% CO_2. The composition of the ACSF was as follows (in mM): 124 NaCl, 2.5 KCl, 1.25 NaH_2PO_4, 2.5 $CaCl_2$, 2 $MgSO_4$, 10 dextrose, and 26 $NaHCO_3$.

Whole-cell recordings

Slices were transferred to a recording chamber (Warner Instruments), and cells were visualized using a Zeiss Axioskop 2 FS Plus microscope

fitted with a 60× water-immersion objective. Whole-cell recordings were conducted using a borosilicate glass micropipette fashioned on a P-97 puller (Sutter Instrument). The resistance of the electrodes was 3–8 MΩ when filled with an intracellular solution of the following (in mM): 130 K-gluconate, 5 NaCl, 10 Na-phosphocreatinine, 1 $MgCl_2$, 0.02 EGTA, 10 HEPES, 2 MgATP, 0.5 Na_2GTP, and 0.1% biocytin, pH 7.3. Dorsal raphe (DR) recordings were confined to the ventromedial DR subdivision that contains the densest cluster of serotonin (5-HT) neurons and were analyzed using pCLAMP software (Molecular Devices) and Clampfit 10.0 (Molecular Devices) as previously described (Beck et al., 2004; Crawford et al., 2010). The cell characteristics measured were resting membrane potential, input resistance, time constant, action potential, and afterhyperpolarization (AHP) characteristics, and voltage–current relationship. To evaluate 5-HT_{1A} receptor responses, slices were stimulated by bath application of a saturating concentration of the nonselective 5-$HT_{1A/1B/7}$ agonist 5-carboxamidotryptamine (5-CT) (100 nM) under voltage-clamp conditions (−60 mV) and the outward currents were measured. We have previously characterized outward currents produced by 5-CT in the dorsal raphe nuclei and excluded the contribution of 5-HT_7 receptors to this response under our recording conditions (Lemos et al., 2006).

Cell filling and morphological analysis

Neurons were filled with 1% biocytin during whole-cell recording and were processed for immunohistochemical detection as described previously (Calizo et al., 2011). No cell was included in the study if it could not be conclusively identified as 5-HT-containing by IHC. A 20× objective lens and optical *z*-slices of 0.8 μm thickness were used to capture the entire extent of the dendritic tree. Confocal stacks were then analyzed using Neurolucida (version 8 and version 9; MBF Bioscience). The cell soma and dendrites were traced using the autoneuron feature and then manually edited if necessary to ensure accurate tracing. Neuron soma characteristics included enclosed volume, surface area, mean length, total cross-sectional area, and mean cross-sectional area. The dendrite parameters included the number of nodes or branch points, the number of ends, the total dendrite length, and the mean dendrite length. In addition, data were obtained for number of branches, total length, and mean length according to branch order. A dendrogram was generated for each cell to obtain the length of the longest segment and the longest soma-to-tip dendritic length. Sholl analysis was performed using radial shells at 20 μm intervals.

Cell culture studies

RN46A cells (White et al., 1994; Bethea et al., 2003) were seeded on glass coverslips in media containing charcoal-stripped hormone-free serum (Sigma-Aldrich). This precaution was taken to prevent corticosteroids present in the serum from confounding the effects of exogenously applied hormones. Twenty-four hours after seeding, cells were pretreated with 5 μM trichostatin A (TSA) (Sigma-Aldrich), 1 mM sodium butyrate (NaBu) (Thermo Fisher Scientific), 10 μM tubacin (provided by Stephen Haggarty and Ralph Mazitschek, Harvard University, Cambridge, MA), or vehicle for 4 h. Cells were then stimulated with 1 μM dexamethasone (DEX) (Sigma-Aldrich) or vehicle for 1 h. After drug treatments, cells were fixed with 4% paraformaldehyde in PBS at 37°C for 20 min, and then permeabilized in 0.1% Triton X-100 in PBS for 5 min at room temperature. After permeabilization, cells were blocked in PBS/2% donkey serum for 1 h. Cells were incubated overnight at 4°C in GR (H-300) antibody (Santa Cruz Biotechnology). The next day, cells were washed with PBS, treated for 1 h at room temperature with Cy3-donkey anti-rabbit secondary antibody (Jackson ImmunoResearch), washed again with PBS, and mounted onto slides using ProLong Gold antifade reagent (Invitrogen). Slides were incubated overnight and imaged the next day on a fluorescent microscope using NIS Element software (Nikon). Line averaging was used to determine fluorescence intensity across each cell, and values were averaged for each cell for the nucleus and for the cytoplasmic region.

Hsp90 coimmunoprecipitation studies

Brain tissues collected from $HDAC6^{NestinCre}$ KO and WT mice were immediately homogenized in 1× RIPA buffer (Millipore) plus protease inhibitor mixture (Roche). A total of 250 μg of lysate was diluted to a concentration of 1 μg/μl in RIPA buffer and incubated with 1 μg of Hsp90 antibody (StressMarq) tumbling overnight at 4°C. Samples were then incubated with 40 μl of protein G beads (Santa Cruz Biotechnology) for 2 h at 4°C while tumbling. Beads were washed twice with RIPA buffer and once with 1× PBS, and eluted in 2× loading buffer (Invitrogen). Proteins were separated using electrophoresis, transferred to a nitrocellulose membrane, and probed for total Hsp90 (GeneTex), AcHsp90 (K294) (Rockland Immunochemicals), or GR (Santa Cruz Biotechnology).

Nuclear fractionation and GR measurement

Mice were subjected to a 10 min social defeat, and 30 min later dorsal raphe punches were taken immediately following removal of the brain. Tissue was homogenized in 1× PBS containing protease inhibitor mixture, and cytoplasmic and nuclear fractions obtained using a commercially available kit (BioVision). Fractions were separated by gel electrophoresis followed by immunoblotting as described above. Efficiency of nuclear fractionation was confirmed using histone H3 and α-tubulin as nuclear and cytoplasmic markers, respectively.

Western blotting

A standard Western blotting protocol (4–20% SDS-PAGE) was used to assess total and acetylated α-tubulin (6-11B-1; Sigma-Aldrich; 1:2000), acH3K14 (Millipore; 1:1000), acH4 (Millipore; 1:2000), and acH3K9 (Cell Signaling) with β-Actin (MP Biomedicals; 1:40,000) as a loading control. Western blots were quantified using the Odyssey system (LI-COR).

Gene expression studies

To examine the regulation of HDAC6 mRNA levels with social defeat and imipramine, DR neurons were collected from male ePet-YFP mice in which a yellow fluorescent tag is placed under the control of the serotonin-specific transcription factor Pet1 (Scott et al., 2005). Laser capture microdissection (LCM) was conducted using an ArcturusXT System (MDS Analytical Technologies). Six animals were used per condition and 500–1000 cells were collected per animal. RNA was extracted from LCM-collected cells and submitted to two rounds of linear amplification using K294WT ovation kit (NuGEN). Amplified RNA had 260/280 and 260/230 ratios >1.8 and Agilent bioanalyzer confirmed RNA quality (RNA integrity number) was excellent (>9.3). Relative mRNA levels for the serotonergic marker TPH normalized to GAPDH were 4×10^4-fold higher in DR LCM samples than in samples collected in regions immediately surrounding the DR on the same slides, and approximately fourfold higher than in conventional DR punch dissections, thus confirming successful enrichment of 5-HT neurons. Before sample collection, ePet-YFP mice were subjected to a social defeat procedure or control condition for 10 d and were screened in a social interaction test, as described above. Based on individual interaction ratios, mice were categorized as vulnerable or resilient and were distributed across vehicle or imipramine (20 mg/kg, i.p.) treatment conditions. Imipramine treatment was given for daily for 28 d following social defeat. Tissues were collected 24 h after the last injection. We have shown previously that this regimen of imipramine restores social interaction to control levels in vulnerable mice but is devoid of behavioral effect in control and resilient mice (Berton et al., 2006).

To compare the regulation of GR target genes in WT and HDAC6 KOs following subchronic GR stimulation, mice were injected with dexamethasone (Sigma-Aldrich) at 1 mg/kg, intraperitoneally, daily for 4 d between 8:00 and 10:00 A.M., and killed 6 h following the final injection. Brains were rapidly removed and frozen in a dry ice/isopentane bath. Punches of DR of ~1 mm^3 were obtained on a cryostat and RNA isolated using the RNAqueous-4PCR kit (Ambion). RNA was converted to cDNA using the SuperScript II First Strand Synthesis system (Invitrogen), and quantitative PCR (qPCR) was performed using SYBR Green technology. Percentage change was calculated using the ΔΔCt method. All samples were run in triplicate and normalized to two housekeeping genes, GAPDH and HPRT. The following primers were used: HDAC6, forward, CAG CAC ACT TCT TTC CAC CAC, and HDAC6, reverse, TCC ACC GGC CAA GAT TCT TCT; TPH2, forward, GGT TGT CCT TGG ATT

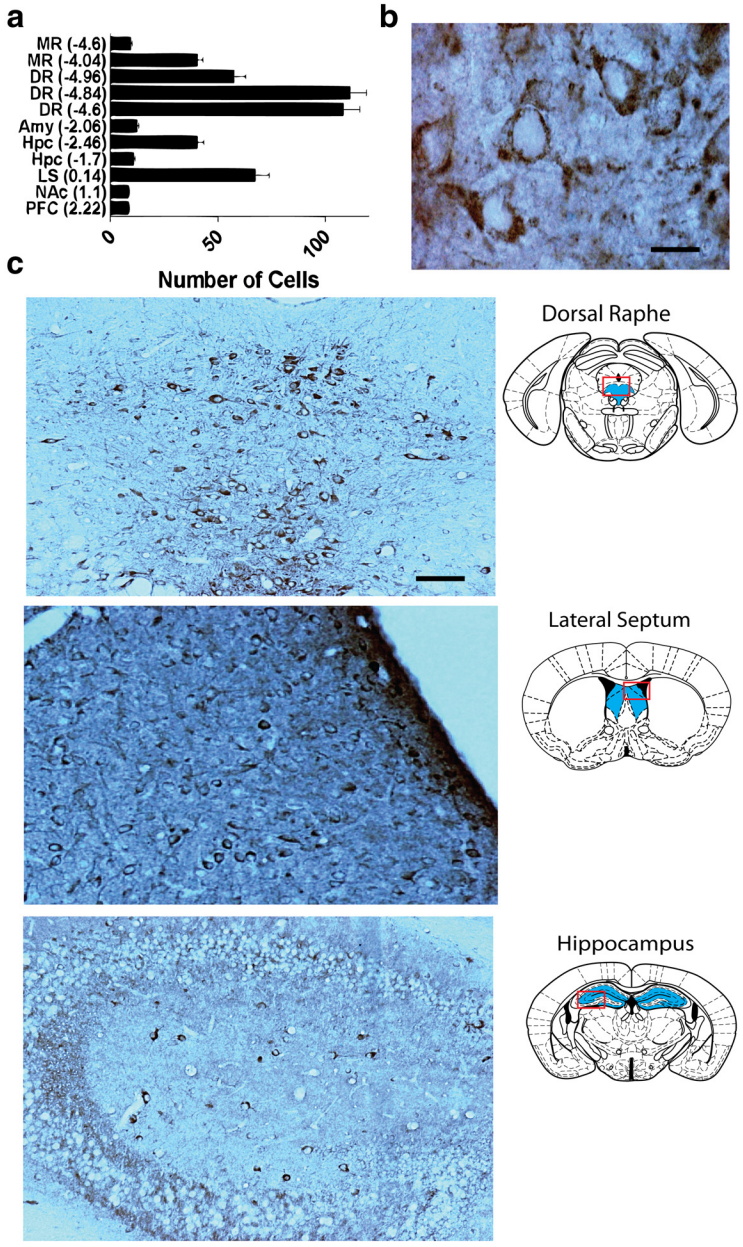

Figure 1. Distribution of HDAC6-immunopositive cells in the mouse brain. ***a***, Number of HDAC6-immunopositive cell bodies per brain area determined from coronal slices. The numbers in parentheses on the *y*-axis are the distance to bregma in millimeters ($n = 4$ mice). MR, Median raphe; DR, dorsal raphe; Amy, amygdala; Hpc, hippocampus; LS, lateral septum; NAc, nucleus accumbens; PFC, prefrontal cortex. ***b***, High-magnification picture illustrating the cytoplasmic pattern of HDAC6 immunostaining. ***c***, Low-magnification pictures illustrating the distribution of HDAC6-positive cells in the three areas where highest number of cells are encountered. Scale bar, 300 μm. Error bars indicate SEM.

CTG CTG, and TPH2, reverse, GCC TGG ATT CGA TAT GAA GCA; 5HT-1A, forward, GAC AGG CGG CAA CGA TAC T, and 5HT-1A, reverse, CCA AGG AGC CGA TGA GAT AGT T; serum glucocorticoid-regulated kinase (SGK), forward, CTG CTC GAA GCA CCC TTA CC, and SGK, reverse, TCC TGA GGA TGG GAC ATT TTC A; FKBP5, forward, TGA GGG CAC CAG TAA CAA TGG; FKBP5, reverse, CAA CAT CCC TTT GTA GTG GAC AT; GAPDH, forward, AAC TTT GGC ATT GTG GAA GG; GAPDH, reverse, GGA TGC AGG GAT GAT GTT CT; HPRT, forward, CAA AGC CTA AGA TGA GCG CAAG, and HPRT, reverse, TTA CTA GGC AGA TGG CCA CAG.

Statistics

All variables were distributed normally and were analyzed using parametric statistics (i.e., one-, two-, or three-way ANOVAs with repeated measures, followed by Fisher's PLSD tests where appropriate). In one instance, ANOVA could not be used as the skewed distribution of interaction scores in HDAC6 KOs led to an incomplete factorial design. In this experiment testing the effect of resilience on morphological variables (see Fig. 8), multiple group comparisons were conducted using Kruskal–Wallis tests. Correlations between pairs of variables were examined using linear regressions and proportions were compared using the Fisher exact test. Statistical significance was defined as a value of $p < 0.05$, and all data are presented as the mean ± SEM.

Results

HDAC6 is enriched in serotonin neurons

To map distribution of HDAC6, we performed IHC and *in situ* hybridization (ISH) on serial mouse brain sections. For IHC, we obtained robust cytoplasmic staining (Fig. 1) with clear regional distribution in the mouse brain using a custom affinity-purified antibody raised against amino acids 991–1149 of murine HDAC6 (Gao et al., 2007). Stereological counts of the number of labeled somas identified the midbrain raphe nuclei as the area with the densest populations of HDAC6-immunopositive cells. In addition to the raphe, numerous HDAC6-immunopositive cell bodies were also detected in a portion of the ventromedial forebrain comprising the subventricular zone and the lateral septum and in the dorsal hippocampus. Dual labeling showed that 97% HDAC6$^+$ DR neurons were positive for the neuronal marker NeuN (194 of 200), while none (0 of 174) were colabeled for the astroglial marker GFAP, a result indicating that the HDAC6-immunopositive cell population in this area is composed exclusively of neurons in adult mice (Fig. 2).

Analysis of HDAC6 distribution by ISH (Figs. 1*a*, 2*a*) revealed a mRNA pattern consistent with that of HDAC6 protein. A search conducted using the Allen Brain Atlas (http://www.brain-map.org) revealed a strong correlation between the distribution of HDAC6 mRNA and that of the serotonergic marker tryptophan hydroxylase 2 (TPH2) (Allen Brain Atlas; NeuroBlast score, 0.70) (Allen Institute for Brain Science et al., 2008). No such overlap was observed for any other HDAC isoforms in the midbrain, including HDAC4 and HDAC10, the two isoforms most structurally related to HDAC6. Dual-label IHC revealed colocalized TPH signal in 94% (283 of 300) of HDAC6-positive cells. In contrast, HDAC6 immunolabeling was not observed in midbrain TH (tyrosine hydroxylase)-positive cells in the ventral tegmental area and substantia nigra or locus ceruleus (data not shown). To determine whether the enrichment of HDAC6 in 5-HT neurons is conserved across species, we examined the expression of HDAC6 in human postmortem DR

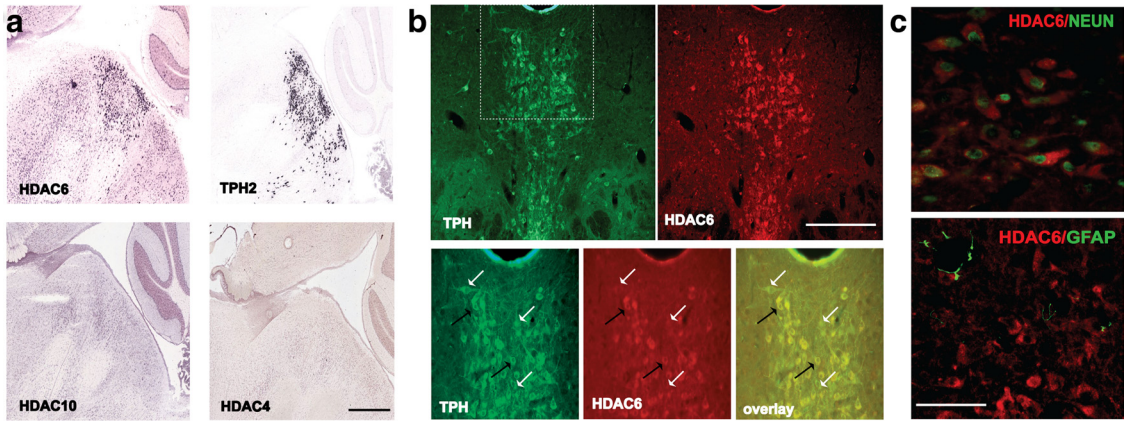

Figure 2. HDAC6 is enriched in serotonin neurons. ***a***, Overlapping pattern of HDAC6 and TPH2 mRNA expression on a sagittal view of the mouse DR. This pattern is specific to HDAC6 and was not observed for other class II HDACs such as HDAC4 or the highly homologous class IIb HDAC10. Scale bar, 300 μm. Pictures are courtesy of the Allen Mouse Brain Atlas (Allen Institute for Brain Science; http://mouse.brain-map.org). ***b***, High degrees of cellular colocalization between HDAC6 signal (red) and the serotonergic marker TPH (green). The region located ventrally to cerebral aqueduct (indicated by dotted line on the top left image) is magnified on the three bottom images. Approximately 95% of HDAC6$^+$ cells found in the dorsal raphe were also positive for TPH (black arrows). The white arrows indicate TPH-positive cells that were negative for HDAC6. Scale bar, 300 μm. ***c***, Dual-labeling IHC for HDAC6 showed colocalization with the neuronal marker NeuN and absence of colocalization with the astroglial marker GFAP. Scale bar, 50 μm.

and observed similar colocalization with TPH as seen in the mouse (data not shown).

Downregulated HDAC6 expression in the dorsal raphe of resilient and imipramine-treated mice

Recent studies have reported the abnormal expression of several HDACs, including HDAC6, in patients with mood disorders (Covington et al., 2009; Hobara et al., 2010). To test whether the expression of HDAC6 in serotonin neurons is altered in a mouse model of stress-related disorders and treatment, we quantitated HDAC6 mRNA in the DR using qPCR. Tissues were collected using LCM in male ePet-YFP mice exposed to chronic social defeat for 10 d and subsequently treated for 28 d with the antidepressant imipramine (20 mg/kg) or vehicle. We have shown previously that this imipramine regimen restores social interaction to control levels in social defeat vulnerable mice, while it is devoid of behavioral effects in control animals (Berton et al., 2006). Statistical analysis revealed a significant main effect of treatment condition ($F_{(3,25)} = 6.55$; $p = 0.0025$). While there was no change in HDAC6 expression after social defeat in vulnerable mice treated with vehicle, we observed a significant 30–40% downregulation of HDAC6 in mice spontaneously expressing resilient phenotype as well as in vulnerable mice treated with imipramine (Fisher's PLSD, $p < 0.01$; $n = 6–8$) (Fig. 3*b*).

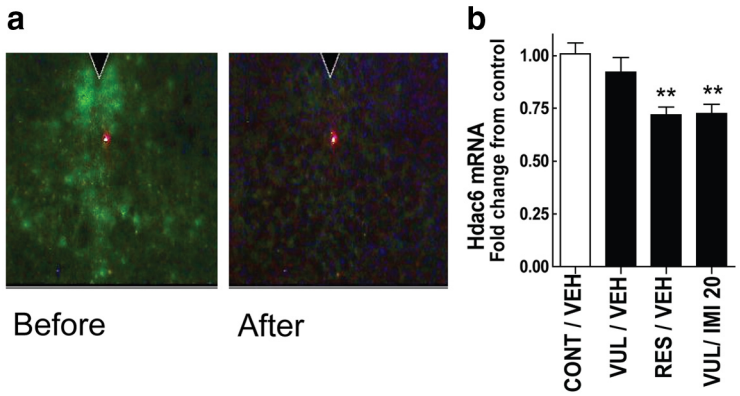

Figure 3. Downregulation of HDAC6 in 5-HT neurons with imipramine and resilience. ***a***, Pictures taken before and after laser capture microdissection of 5-HT neurons from a 10-μm-thick coronal slice of the dorsal raphe nucleus in ePet-YFP transgenic mice. The white triangle indicates the position of the cerebral aqueduct. ***b***, HDAC6 mRNA levels measured by qPCR. Note the absence of regulation of HDAC6 in vulnerable animals receiving vehicle (VUL/VEH), and the significant downregulation of HDAC6 in resilient mice treated with vehicle (RES/VEH) as well as in vulnerable mice treated with 20 mg/kg imipramine (VUL/IMI) ($n = 6–8$ per condition; $^{**}p < 0.01$ vs CONT/VEH). Error bars indicate SEM.

Conditional ablation of HDAC6 in raphe neurons

The enrichment of HDAC6 in 5-HT neurons positions it as a potential regulator of threat-related and socioaffective behaviors (Dayan and Huys, 2009). To test this hypothesis, we genetically depleted HDAC6 by taking advantage of a previously characterized floxed HDAC6 allele from which we derived two lines of mice lacking HDAC6, either selectively in 5-HT neurons (HDAC6^{Pet1Cre} KO) or in a pan-neuronal manner (HDAC6^{NestinCre} KO). In HDAC6^{Pet1Cre} KO mice, we observed a loss of HDAC6 mRNA signal by ISH (Fig. 4*a*) and a decrease of 85–90% in the total number of HDAC6-immunopositive neurons across the entire rostrocaudal extent of the raphe nucleus (Fig. 4*a*). These results confirm genetically that the vast majority of HDAC6-immunopositive neurons in the raphe are serotonergic. We detected a small proportion of spared HDAC6-immunopositive neurons in the raphe nuclei of HDAC6^{Pet1Cre} KOs. These spared neurons were all TPH$^+$ and represented 10–15% of the total number of TPH$^+$ cells per slice (Fig. 4*a*, inset). This observation is in good agreement with several reports indicating that a corresponding proportion of 5-HT neurons in raphe does not express the Pet1 gene (Braz et al., 2009; Kiyasova et al., 2011). Counts of HDAC6-immunoreactive somas throughout the brain indicated that the depletion HDAC6 in HDAC6^{Pet1Cre} KO mice was restricted to the raphe nuclei and did not extend to forebrain regions expressing HDAC6.

To evaluate the influence of HDAC6 on protein lysine acetylation in the DR, we measured bulk levels of acetylated histone and non-histone proteins in this area. We first examined acetylation of α-tubulin at lysine 40, a well characterized substrate of HDAC6

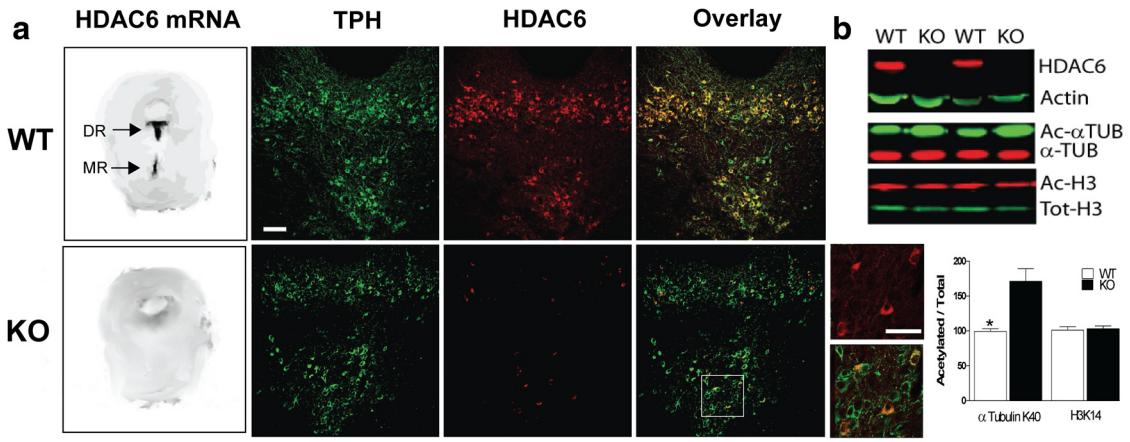

Figure 4. Depletion of HDAC6 in raphe nuclei leads to hyperacetylation of α-tubulin but not histone H3. Histological studies confirm that HDAC6 transcript and protein are depleted in a serotonin-selective manner in HDAC6^{Pet1Cre} KO mice. ***a***, HDAC6 ISH and IHC signal on coronal views of the brainstem in WT and HDAC6^{Pet1Cre} KO mice. The left column depicts ISH autoradiographs. The two areas with dense HDAC6 signal in the midline portion of the WT slice correspond to the DR and median raphe (MR) nuclei. Note how this signal is lost in HDAC6^{Pet1Cre} KO mice. The right columns show fluorescent views of the DR in WT and HDAC6^{Pet1Cre} KO after dual IHC for HDAC6 (red) and TPH (green). Note how the vast majority of colocalized HDAC6/TPH signal appearing in yellow on overlay in the WT view is lost in the HDAC6^{Pet1Cre} KO, while TPH signal remains intact. Scale bar, 100 μm. The higher-magnification insets illustrate the small proportion of spared HDAC6/TPH-immunopositive cells in HDAC6^{Pet1Cre} KO mice. Scale bar, 50 μm. ***b***, Western blots from dorsal raphe homogenates indicated that pan-neuronal depletion of HDAC6 leads to α-tubulin (K40) hyperacetylation but does not alter acetylation of histone H3 (K14). Levels of HDAC6 were normalized to β-actin levels that did not vary significantly across genotypes. Acetylation was normalized to control values (*$p < 0.05$; $n = 3$–4 per condition). Error bars indicate SEM.

Table 1. Effect of HDAC6 depletion on the distribution, morphology, serotonin synthesis/metabolism, and intrinsic electrophysiological properties of serotonergic neurons: cell body/axon density

	DR somas (nb)	MR somas (nb)	DR TPH (WB)	MR TPH (WB)	DG fibers (% area)	pfCTX fibers (% area)	NAc fibers (% area)
WT	3856 ± 412.6	1433 ± 134.2	100.0 ± 21.31	100.0 ± 11.21	15.26 ± 0.70	7.03 ± 0.50	16.21 ± 0.12
KO	3692 ± 601.6	1527 ± 201.6	127.8 ± 10.8	102.39 ± 6.8	11.04 ± 2.13	6.58 ± 0.90	15.33 ± 0.42

Lack of difference between behaviorally naïve WT and HDAC6^{Pet1cre} KO mice in number of 5-HT-immunopositive somas in DR and median raphe (MR) nuclei, and the density of 5-HT-immunopositive axons in dentate gyrus (DG), prefrontal cortex (pfCTX), and nucleus accumbens (NAc) estimated stereologically using an optical fractionator and area fraction fractionator probes, respectively (Stereo Investigator software; MBF Bioscience; $n = 3$ mice/condition). Lack of difference in TPH protein levels measured by Western blot in DR and MR ($n = 5$–6 per condition).

Table 2. Effect of HDAC6 depletion on the distribution, morphology, serotonin synthesis/metabolism, and intrinsic electrophysiological properties of serotonergic neurons: somatodendritic morphology

	Soma				Dendrites				
	Volume (μm^3)	Surface area (μm^2)	Mean length (μm)	Mean area (μm^2)	Longest dendrite (μm)	Trees (nb)	Nodes (nb)	Ends (nb)	Mean dendrite length (μm)
WT	3148.4 ± 653.2	954.8 ± 137.3	56.5 ± 2.8	212.9 ± 19.8	321.5 ± 47.5	3.7 ± 0.5	4.0 ± 0.6	272.6 ± 36.4	272.6 ± 36.4
KO	3076.1 ± 672.9	974.7 ± 134	59.6 ± 2.8	229.3 ± 19.4	413.1 ± 64	4.1 ± 0.3	3.4 ± 0.8	324.6 ± 42.2	324.6 ± 42.2

Lack of difference in the detailed morphological characteristics of soma and processes in biocytin-filled 5-HT DR neurons from behaviorally naive WT and HDAC6^{Pet1cre} KO mice ($n = 9$–12 cells, 1 cell/mouse). All cells were collected from the ventromedial portion of the DR confirmed for serotonergic identity and HDAC6 KO using IHC.

(Hubbert et al., 2002; Matsuyama et al., 2002; Haggarty et al., 2003).Western blots from HDAC6^{NestinCre} KO brainstem homogenates revealed a twofold increase in levels of acetylated α-tubulin at lysine 40 compared with WT (Fig. 4*b*). This increase in tubulin acetylation occurred without concomitant changes in the level of acetylated histone H3 at lysine 14 (Fig. 4*b*) and at lysine 9 (WT, 1.32 ± 0.45; KO, 1.07 ± 0.44; $n = 3$) nor of histone H4 (WT, 0.79 ± 0.37; KO, 1.48 ± 0.4; $n = 3$).

Serotonin-selective depletion of HDAC6 does not result in major cellular abnormalities

Loss of function of certain HDAC isoforms is known to produce neurodevelopmental abnormalities in the mouse (Akhtar et al., 2009; Montgomery et al., 2009). To test whether HDAC6 is critical to the development of DR 5-HT neurons, we evaluated the consequences of HDAC6 depletion on their number, morphology, and intrinsic electrophysiological characteristics. Histological, morphological, and electrophysiological evaluations conducted in naive adult WT and HDAC6^{Pet1Cre} KO animals did not reveal any major abnormality (Tables 1–4). Stereological counts of the numbers of 5-HT$^+$ somas in the DR and stereological estimations of the density of 5-HT-immunoreactive axon terminals in several serotonergic projection areas indicated that gross morphological features of 5-HT ascending pathways were preserved in the absence of HDAC6. Finer morphological analyses conducted in 5-HT neurons individually filled with biocytin and reconstructed using the Neurolucida software also revealed a lack of significant alterations in somatodendritic morphology and complexity of 5-HT neurons (Table 2). Evaluation of the levels of 5-HT and its major metabolite 5-hydroxyindoleacetic acid (5-HIAA) in raphe tissues or major projection areas did not reveal any significant abnormalities in the ability of HDAC6-deficient neurons to synthesize and metabolize serotonin (Table 3). The sole significant cellular abnormality found in HDAC6^{Pet1Cre} KO compared with WT mice under baseline conditions was a 50% decrease in membrane resistance of serotonin neurons (effect of genotype, $F_{(1,59)} = 4.92$, $p = 0.002$; Fisher's PLSD, $p < 0.01$) detected using whole-cell recordings in acute DR slices. However, HDAC6^{Pet1Cre} KO mice had normal resting membrane

Table 3. Effect of HDAC6 depletion on the distribution, morphology, serotonin synthesis/metabolism, and intrinsic electrophysiological properties of serotonergic neurons: serotonin synthesis/metabolism

	5-HT (pg/mg)				5-HIAA (pg/mg)			
	MR	DR	HPC	pfCTX	MR	DR	HPC	pfCTX
WT	254.7 ± 28.6	338.4 ± 24.5	237.8 ± 13.0	89.0 ± 12.5	150.7 ± 11.8	116.7 ± 12.0	120.6 ± 10.8	30.1 ± 2.4
KO	224.8 ± 25.8	316.3 ± 23.8	224.3 ± 22.7	89.4 ± 8.5	131.4 ± 12.0	111.2 ± 12.4	92.0 ± 13.1	29.1 ± 2.4

Lack of changes in tissue levels of serotonin and its metabolite 5-HIAA (in picograms per milligram) determined by HPLC in HDAC6^{Pet1cre} KO mice compared with WT mice. $n = 6–8$/group. MR, Median raphe; DR, dorsal raphe; HPC, hippocampus; pfCTX, prefrontal cortex.

Table 4. Effect of HDAC6 depletion on the distribution, morphology, serotonin synthesis/metabolism and intrinsic electrophysiological properties of serotonergic neurons: intrinsic electrophysiological properties

	RMP (mV)	Resistance (MΩ)	τ (ms)	AP threshold (mV)	AP amplitude (mV)	AP duration (ms)	AHP amplitude (mV)	AHP $t_{1/2}$ (ms)	Activation gap (mV)	5-CT response (%)
WT	−56 ± 3.6	632 ± 81.4	36 ± 4	−28 ± 1.1	66 ± 4.6	3 ± 0.1	−25 ± 1.4	303 ± 44.2	29 ± 2.9	100 ± 2
KO	−62 ± 2.8	381 ± 35.4^{++}	36 ± 5.3	−29 ± 1.1	69 ± 2.9	3 ± 0.4	−30 ± 1.5	309 ± 30.7	33 ± 2.8	100 ± 1

Electrophysiological characteristics of DR neurons in naive WT and HDAC6^{Pet1cre} KO mice. $n = 10–11$ cells per condition. Note the significant reduction in membrane resistance in HDAC6^{Pet1cre} KO.
$^{++}p < 0.01$, compared with WT.

Table 5. Effect of HDAC6 depletion on the behavioral phenotype of naive mice: basic physiology/locomotion

	Food intake (g/d)	Water intake (ml/d)	Rotarod latency to fall (s)	Locomotor activity—ambulation	Locomotor activity—rearing
WT	4.1 ± 0.2	5.9 ± 0.5	59 ± 6	3762 ± 255	200 ± 22
KO	4.2 ± 0.2	5.2 ± 0.3	69 ± 6	4111 ± 175	227 ± 12

HDAC6^{Pet1Cre} (KO) mice and their WT littermates were subjected to variety of behavioral tests. Daily food and water intake was measured for 1 week, and locomotor coordination and activity were measured in the rotarod test and locomotor activity boxes. No significant differences were noted in average food or water intake, latency to fall from the rotarod, or total ambulation or rearing in the locomotor boxes.

potential, time constant (τ), action potential amplitude, threshold, and width (Table 4).

Serotonin-selective depletion of HDAC6 does not result in major behavioral abnormalities in naive mice

To evaluate the behavioral impact of HDAC6 depletion in 5-HT neurons, male HDAC6^{Pet1Cre} KO mice and their WT littermates were compared in a comprehensive phenotyping screen conducted in 8- to 10-week-old behaviorally naive mice. This screen did not reveal any significant alteration of basic physiological or behavioral functions such as food and water intake, motor coordination, locomotor activity patterns, social interest, anxiety, and startle responses (Tables 5–7).

Serotonin-selective depletion of HDAC6 promotes an antidepressant-like phenotype in mice exposed to inescapable stress

The only two behavioral tests in which significant genotype-dependent differences were observed in previously unmanipulated mice were the TST and the FST, where active escape behaviors are assessed in response to acute inescapable stressors (Fig. 5*a*,*b*). Both of these measures are classically used as endpoints to evaluate antidepressant activity upon acute administration (Cryan et al., 2002). In these two tests, HDAC6^{Pet1Cre} KO mice displayed a modest antidepressant-like phenotype characterized by a reduction in the time spent immobile compared with their WT littermates (Fig. 5*a*,*b*; for TST, $F_{(1,16)} = 5.29$, $p = 0.04$; for FST, $F_{(1,22)} = 4.79$, $p = 0.04$).

We next evaluated whether depletion of HDAC6 in serotonin neurons influences resilience to chronic stress in the social defeat model (Fig. 5*c–e*), a paradigm that responds to chronic but not acute antidepressant administration. Social defeat induced a dramatic downward shift in the distribution of individual interaction ratios (Fig. 5*d*) and in the absolute time spent in the interaction zone (Fig. 5*e*) in WT mice, but it had no significant effect on these variables in HDAC6^{Pet1Cre} KO mice (genotype by defeat interaction on interaction ratios, $F_{(1,149)} = 5.47$; $p < 0.05$, Fisher's PLSD in WT group, $p < 0.001$; genotype by defeat interaction on time in interaction zone, $F_{(1,149)} = 5.78$; $p < 0.05$, Fisher's PLSD in WT, $p < 0.01$). In WT animals, 31% of the mice tested were categorized as resilient after social defeat, while 45% displayed strong social avoidance (interaction ratio, <50). In contrast, a higher proportion of HDAC6^{Pet1Cre} KO mice (50%) was classified as resilient and only 23% developed strong avoidance (Fisher's exact test, $p < 0.01$). Importantly, there was no difference between undefeated WT and HDAC6^{Pet1Cre} KO regarding interaction ratios (WT, 177.86 ± 19.34%; KO, 142.25 ± 17.79%; NS) or absolute time spent in the interaction zone (WT, 61.94 ± 6.29 s; KO, 50.90 ± 4.82 s; NS), indicating that serotonergic depletion of HDAC6 does not interfere with baseline expression of social investigation behaviors. Rather, the finding that HDAC6^{Pet1Cre} KO mice fail to display the typical social avoidance response after social defeat suggests that HDAC6 in serotonin neurons may play a role in the experience-dependent modulation of socioaffective responses.

Depletion of HDAC6 prevents social defeat-induced hypoexcitability of serotonin neurons

Because the behavioral phenotype of HDAC6^{Pet1Cre} KO mice emerges primarily after exposure to inescapable stressors, we reasoned that the neurobiological influence of HDAC6 may also become more readily observable under these conditions. We thus extended our previous electrophysiological analyses in HDAC6^{Pet1Cre} KO and WT mice by incorporating slices from animals exposed to 10 d of social defeat. Raphe brain slices were collected for whole-cell recordings 24 h after the last exposure to social defeat or control conditions. To correlate resiliency status with cell properties, control and defeat-exposed mice were tested for social avoidance immediately before tissue collection. Recorded neurons were sampled exclusively from the ventromedial subfield of the DR, and their 5-HT phenotype was confirmed postrecording using TPH immunohistochemistry (data not shown). In WT mice, social defeat had a profound impact on physiological properties of 5-HT neurons. First, we observed a robust defeat-induced hypoexcitability in 5-HT cells, as revealed by frequency–intensity plots (Fig. 6*a*,*b*). When exposed to the same input current, 5-HT neurons of defeated WT mice consis-

Table 6. Effect of HDAC6 depletion on the behavioral phenotype of naive mice: sociability and anxiety

	Social investigation test		Elevated plus maze			
	Duration of social investigation (s)	Latency to social investigation (s)	Open arm time (s)	Closed arm time (s)	Open arm entries	Closed arm entries
WT	136.39 ± 11.97	10.71 ± 2.96	13.79 ± 4.71	218.47 ± 10.74	6 ± 1	23 ± 2
KO	108.71 ± 14.51	8.26 ± 3.11	15.00 ± 4.79	215.82 ± 11.68	7 ± 1	23 ± 2

HDAC6^{Pet1Cre} (KO) mice and their WT littermates were subjected to a variety of behavioral tests. Mice were tested for social exploration and anxiety in social choice and elevated plus maze tasks. No significant differences were noted in time spent investigating a juvenile social target or latency to investigate the target, or in time spent in or entries into either the open or closed arms of the plus maze.

Table 7. Effect of HDAC6 depletion on the behavioral phenotype of naive mice: startle responses

	Acoustic startle								Prepulse inhibition (% PPI)		
	Baseline (0 db)	90 db	95 db	100 db	105 db	110 db	115 db	120 db	60 db	73 db	81 db
WT	4 ± 1	10 ± 2	12 ± 2	23 ± 4	41 ± 7	74 ± 15	97 ± 24	92 ± 22	30 ± 7	41 ± 10	53 ± 7
KO	6 ± 3	14 ± 2	12 ± 4	22 ± 6	37 ± 8	61 ± 10	65 ± 11	75 ± 15	20 ± 13	40 ± 11	57 ± 6

HDAC6^{Pet1Cre} (KO) mice and their WT littermates were subjected to variety of behavioral tests. Startle responses were measured in both baseline acoustic and prepulse inhibition tests. No differences in startle responses were observed at any stimulus or prepulse intensity. $n = 8$–9 for all tests.

tently fired at frequencies 50% lower than those of controls. This difference was significant for input current steps ranging from 40 to 80 pA (Fig. 6*b*, social defeat by genotype interaction, $F_{(1,59)} = 7.3$, $p = 0.009$; Fisher's PLSD, $p < 0.05$). Second, we found that both the AHP amplitude (Fig. 6*c*) and activation gap [the difference between the resting membrane potential (RMP) and action potential (AP) threshold] were significantly increased by defeat in WT mice (control, 29.00 ± 2.90 mV; defeat, 41.00 ± 2.40 mV; defeat by genotype interaction, $F_{(1,59)} = 6.29$, $p = 0.01$; Fisher's PLSD, $p < 0.01$). Finally, we evaluated the effect of social defeat on the functional coupling of the 5-HT$_{1A}$ autoreceptor. 5-HT$_{1A}$ receptor responses were triggered by bath application of the 5-HT$_{1A}$ receptor agonist 5-carboxyamidotryptamine maleate (5-CT) (100 nM), and the amplitude of the resulting outward current was measured. We found that, in WT mice, social defeat potentiated 5-HT$_{1A}$ receptor-mediated responses (Fig. 6*d*), while it had no effect on 5-HT$_{1A}$ receptor-mediated responses in raphe slices from HDAC6^{Pet1Cre} KO mice (Fig. 6*e–h*) (defeat by genotype interaction, $F_{(1,50)} = 3.55$, $p = 0.05$; Fisher's PLSD, control vs defeat, $p = 0.05$ in WT). These results indicate HDAC6 in 5-HT neurons mediates the neurophysiological consequences of social defeat stress on 5-HT neurons.

Depletion of HDAC6 prevents social defeat-induced hypertrophy of 5-HT neurons

In conjunction with the electrophysiological changes identified above in 5-HT neurons, certain morphological neuroadaptations may contribute to alter the net functional output of raphe circuits after defeat. To date, however, evidence for such structural changes in raphe neurons after stress or stress hormone exposure has remained relatively indirect (Azmitia et al., 1993; Azmitia and Liao, 1994). Thus, we took advantage of the fact that 5-HT neurons from WT and HDAC6^{Pet1Cre} KO mice exposed to social defeat or control conditions were individually filled with biocytin during whole-cell recordings to test whether changes in the somatodendritic morphology of 5-HT neurons predicted resilience in the social defeat paradigm. Biocytin was processed using fluorescently conjugated streptavidin to visualize neurons, and confocal stacks were collected to generate 3D neuronal reconstructions that were subsequently analyzed using Neurolucida software (Fig. 7*a*).

As summarized by representative drawings in Figure 7*b*, social defeat induced increases in soma size and dendritic complexity of DR 5-HT neurons in WT mice. Significant correlations were observed in defeat-exposed WT mice between the time spent in the interaction zone (target present) and three morphological variables, namely the mean cell body surface (Fig. 6*c*; $R^2 = 0.45$; $p < 0.001$), the cumulative number of Sholl intersections, an index of dendritic complexity (Fig. 6*d*; $R^2 = 0.29$; $p < 0.01$), and the mean dendrite length (Fig. 6*e*; $R^2 = 0.3$; $p < 0.01$). In contrast, no correlations were observed between these variables in controls from both genotypes (data not shown) or in defeat-exposed HDAC6^{Pet1Cre} KO mice, in which expression of social avoidance was reduced, in agreement with our previous observation. When defeat-exposed mice were stratified into vulnerable and resilient subgroups on the basis of their interaction ratios, the rightward shift in the distribution of interaction scores in HDAC6^{Pet1Cre} KOs led to an incomplete factorial design (i.e., lack of KO/vulnerable mice) that impeded the use of parametric statistics. Kruskal–Wallis nonparametric tests revealed significant increases in mean cell body surface (Fig. 6*f*; $H_{(4,45)} = 11.26$; $p < 0.05$), in the mean dendrite length (Fig. 6*h*; $H_{(4,45)} = 10.99$; $p < 0.05$), and in dendritic complexity (Fig. 6*g*; $H_{(4,45)} = 9.58$; $p < 0.05$) in WT vulnerable but not resilient mice. Sholl's analysis conducted along the entire extent of the dendritic tree up to 380 μm from the soma revealed that the increase in cell complexity after social defeat was specific to proximal dendrites found within a 140 μm distance from soma (data not shown; two-way ANOVA, soma distance by social defeat interaction, $F_{(1,19)} = 1.88$, $p < 0.05$).

In summary, our results indicate that social defeat leads to an increased cell body and increased dendritic length and complexity of 5-HT neurons that constitutes a robust morphological biomarker of vulnerability to defeat. Like behavioral and electrophysiological effects of social defeat, these morphological consequences were prevented by serotonergic depletion of HDAC6.

HDAC6 depletion leads to Hsp90 hyperacetylation and impaired GR chaperoning

Having demonstrated that 5-HTergic depletion of HDAC6 opposes the behavioral and certain neuroplastic consequences of social defeat in raphe circuits, we next examined intracellular mechanisms mediating the proresilient effects of HDAC6 depletion. We focused on the GR chaperone protein Hsp90, a well characterized substrate of HDAC6. Hyperacetylation of Hsp90 following pharmacologic or genetic inactivation of HDAC6 has a major inhibitory impact on intracellular responses to glucocorticoids (Kovacs et al., 2005; Murphy et al., 2005; Zhang et al., 2008). Because GR is abundantly expressed in raphe nuclei by both serotonergic and nonserotonergic cells (Fig. 8*a*), we hypothesized that the

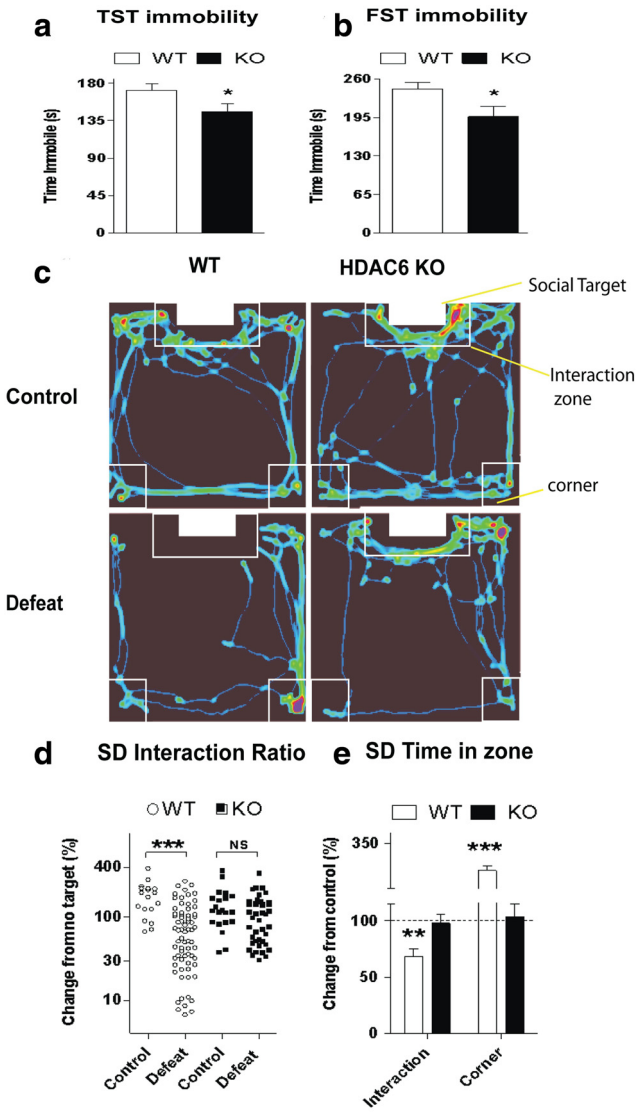

Figure 5. Antidepressant-like phenotype in HDAC6^{Pet1Cre} KO mice. ***a***, ***b***, Decreased immobility of HDAC6^{Pet1Cre} KO compared with WT mice in two despair tests, the TST (***a***) and FST (***b***) (*$p < 0.05$ compared with WT; $n = 15$ per condition). ***c***, Representative videotracking heat maps from WT and HDAC6^{Pet1Cre} KO mice exposed to a social target. The red/yellow colors identify the locations where mice spent the most time. Exposure to chronic social defeat reduced time in the interaction zone in a genotype-dependent manner. Note how high-density traces remain localized to the interaction zone after social defeat in the HDAC6^{Pet1Cre} KO, whereas they shift to the corner zone in the WT. ***d***, Distribution of individual interaction ratios in WT and HDAC6^{Pet1Cre} KO genotypes. Interaction ratios were comparable between control mice of both genotypes (WT, $n = 18$; KO, $n = 21$). Social defeat decreased interaction ratios in WT (control, $n = 18$; defeat, $n = 70$; $p < 0.001$) but had no significant effect in HDAC6^{Pet1Cre} KO mice (control, $n = 22$; defeat, $n = 42$; NS). ***e***, Time spent by defeated mice in the interaction zone versus corner zones of the arena in the "target present" condition. Scores of defeated WT and HDAC6^{Pet1Cre} KO are normalized to controls within each genotype. WT mice decreased their average time in the interaction zone and correspondingly increased their time spent in the corners of the arena distant from the social target. In contrast, no significant defeat-induced change was observed in HDAC6^{Pet1Cre} KO mice (**$p < 0.01$, ***$p < 0.001$, compared with controls). Error bars indicate SEM.

proresilient effects of HDAC6 depletion may result, at least in part, from an inhibition of GR responses in 5-HT circuits.

To test whether resilience to social defeat, which is associated with HDAC6 downregulation in the DR, also correlates with hyperacetylation of Hsp90, we measured Hsp90 acetylation by IHC. Several acetylation sites have been previously identified in Hsp90 (Yang et al., 2008; Choudhary et al., 2009). We examined a specific site (lysine 294) that is directly involved in the ability of Hsp90 to recruit clients and cochaperones (Scroggins et al., 2007) and to promote folding of steroid hormone receptors (Ai et al., 2009; Kekatpure et al., 2009), using an antibody that specifically recognizes the acetylated form of Hsp90 at K294. Cell counting in fields of view sampled across the entire rostrocaudal axis of the raphe revealed a strong trend toward an increase in the average number of raphe cells immunopositive for acHSP90 after social defeat in resilient compared with vulnerable mice (resilient, 38 ± 7; vulnerable, 20 ± 2 cells; $p = 0.06$; $n = 3$).

We then asked whether the role of HDAC6 as a modulator of GR responses, previously established in cultured fibroblasts (Kovacs et al., 2005; Murphy et al., 2005; Zhang et al., 2008), and in the liver *in vivo* (Winkler et al., 2012), extends to serotonin neurons. To accomplish this, we used an immortalized rat raphe neuronal precursor cell line (RN46A) that expresses steroid receptors (White et al., 1994; Bethea et al., 2003). In this cell line, we compared the ability of three HDAC inhibitors, with varying affinity for HDAC6, to antagonize GR translocation following hormonal stimulation. To induce GR translocation, cells were treated with 1 μM DEX for 1 h and were subsequently fixed and immunostained for GR. Relative distribution of GR fluorescence across the nucleus and cytoplasm of individual cells was quantified. To examine the modulation of GR responses by HDAC inhibitors, cells were pretreated with vehicle or TSA (5 μM), NaBu (1 mM), or tubacin (10 μM), for 4 h before GR stimulation. DEX led to an increase in relative nuclear GR signal that reflects the movement of GR from the cytoplasm to the nucleus ($F_{(1,178)} = 30.0$; $p < 0.0001$). This effect was significantly attenuated by pretreatment with TSA ($F_{(1,107)} = 5.20$; $p = 0.02$) and tubacin ($F_{(1,69)} = 8.87$; $p = 0.004$), two inhibitors with nanomolar affinity for HDAC6 (Bradner et al., 2010), but not by the selective class I inhibitor NaBu ($F_{(1,46)} = 1.89$; $p = 0.18$; Fig. 8*b*,*c*). Treatment with HDAC inhibitors alone had no effect on GR translocation in the absence of DEX.

Having confirmed the influence of HDAC6 on GR signaling in 5-HT neurons under tissue culture conditions, we next evaluated whether a similar function of HDAC6 in the DR can be evidenced *in vivo* in adult mice exposed to a psychosocial stressor. We did so by quantitating defeat-induced nuclear translocation of GR in the DR of WT and HDAC6 KO mice. In WT mice, social defeat exposure induced a robust increase in nuclear GR in the DR that presumably reflected GR activation by endogenous glucocorticoids released during social confrontation (Fig. 8*d*). In striking contrast, there was no significant change in nuclear GR levels after social defeat in mice with pan-neuronal HDAC6 depletion (genotype by treatment interaction, $F_{(1,18)} = 4.95$, $p = 0.04$; WT Fisher's PLSD, $p = 0.002$). GR signal was normalized to levels of histone H3 as a control for loading and fractionation procedures. No differences were observed between genotype and treatment groups in levels of H3. Importantly, plasma corticosterone (Cort) levels were not different between WT and HDAC6 KOs at the same time point after social defeat (WT, 124.7 ± 9.0 ng/ml; KO, 139.7 ± 17.4 ng/ml; $n = 4$), a result suggesting that HDAC6 depletion affects stress resilience via a GR-regulated mechanism autonomous to raphe circuits and independent of hypothalamo-pituitary-adrenocortical (HPA) axis regulatory feedback loops.

We next tested whether depletion of HDAC6 induces hyperacetylation of Hsp90 and alters GR–Hsp90 protein–protein interactions in the brain *in vivo*. Hsp90 was immunoprecipitated from WT and HDAC6 KO brainstem lysates and resulting pull-downs were blotted for AcHsp90 or GR (Fig. 8*e*). Values were

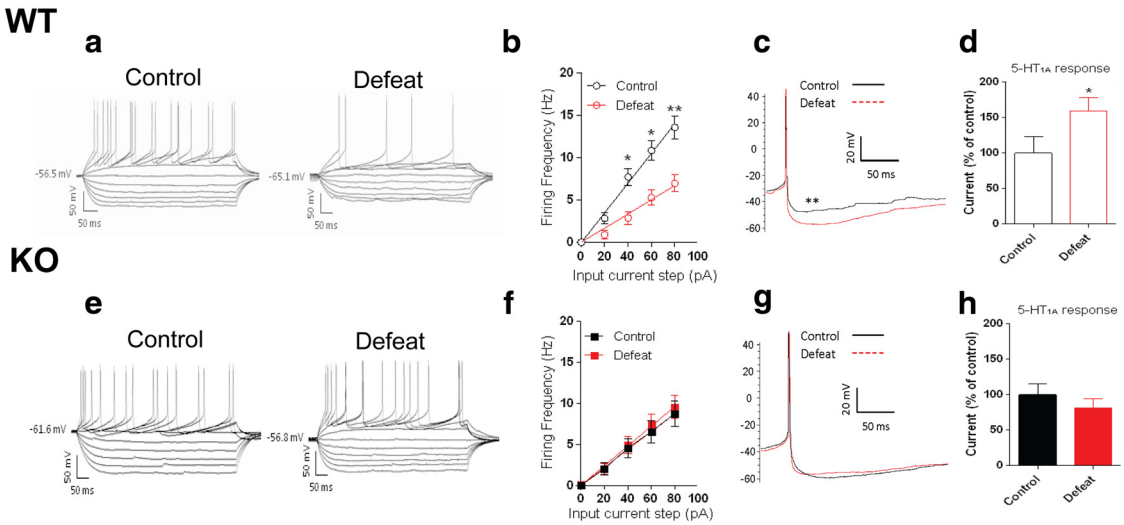

Figure 6. Defeat-induced hypoexcitability of serotonin neurons is prevented by HDAC6 depletion. Whole-cell patch-clamp recordings conducted 24 h after the last defeat in midbrain slices from WT (***a–d***) and HDAC6^{Pet1Cre} KO mice (***e–h***). Representative traces illustrate the hypoexcitability of 5-HT neurons observed after social defeat in WT mice but not HDAC6^{Pet1Cre} KOs (***a***, ***e***). Hyperpolarizing and depolarizing current pulses were injected into recorded cells, and voltage responses were measured. ***b***, ***f***, Corresponding frequency–intensity plots illustrate the reduced firing frequency of WT 5-HT neurons in the 40 – 80 pA range of input currents after social defeat. Note, in contrast, that defeat does not induce a change in the excitability of 5-HT neurons at this range in HDAC6^{Pet1Cre} KO mice. ***c***, ***g***, AHP amplitude was increased by social defeat selectively in WT 5-HT neurons. ***d***, ***h***, Magnitude of outward current following bath application of the 5-HT$_{1A}$ receptor agonist 5-CT (100 nM) was not different between HDAC6^{Pet1Cre} KO and WT mice under control conditions but defeated WT mice responded with greater 5-CT-elicited current than HDAC6^{Pet1Cre} KO mice after social defeat (*$p < 0.05$; **$p < 0.01$, control vs defeat; $n = 11–25$ cells per condition). Error bars indicate SEM.

normalized to the total amount of Hsp90 pulled down. Results from these experiments show that, while total levels of Hsp90 were not altered following neuronal depletion of HDAC6, Hsp90 became hyperacetylated at lysine 294 (optical density: WT, 0.33 ± 0.03; KO, 0.67 ± 0.03; $F_{(1,6)} = 68.95$; $p = 0.0002$; $n = 4$ replicates) and the association between the Hsp90 chaperone and GR was dramatically diminished under these conditions (WT, 0.71 ± 0.09; KO, 0.29 ± 0.09; $F_{(1,4)} = 10.85$; $p = 0.03$; $n = 3$ replicates).

HDAC6 depletion prevents transcriptional and electrophysiological effects of glucocorticoids in 5-HT neurons

Previous studies relying on the use of reporter systems in non-neuronal cells have shown that HDAC6 inactivation blunts GR-mediated transcriptional responses (Kovacs et al., 2005; Zhang et al., 2008). To assess whether HDAC6 KO has a similar functional impact on downstream GR signaling in 5-HT neurons, we evaluated hormone-induced regulation of two well characterized transcriptional targets of GR in this neuronal population, namely the TPH2 and 5-HT$_{1A}$ genes (Ou et al., 2001; Albert and Lemonde, 2004; Clark et al., 2008). To pharmacologically mimic the pulsatile pattern of GR activation with social defeat exposure, WT and HDAC6^{Pet1Cre} KO mice were treated subchronically with DEX (1 mg/kg, i.p.; daily for 4 d) and TPH2 and 5HT$_{1A}$ mRNA levels were evaluated in DR tissues using qPCR. In line with previous literature (Ou et al., 2001; Clark et al., 2008), we observed a repression (35 and 30% decrease, respectively) of TPH2 and 5HT$_{1A}$ gene expression in the DR of WT mice treated with DEX (Fig. 9*a*). In contrast, the same DEX regimen produced no significant effect in HDAC6^{Pet1Cre} KO on the expression of TPH2 (one-way ANOVA, main effect of genotype on DEX-induced change for TPH2, $F_{(1,14)} = 5.53$, $p = 0.03$; and 5HT$_{1A}$, $F_{(1,15)} = 6.61$, $p = 0.02$). These results indicate that HDAC6 is a required mediator of the transcriptional effects of glucocorticoid hormones on these two serotonergic genes. As expected based on cell type selectivity of HDAC6^{Pet1Cre} KO, the genotype dependence of DEX effects did not extend to canonical GR targets genes such as SGK (Fig. 9*a*) or FKBP5 (data not shown), which are ubiquitously expressed by both 5-HT and non-5-HT cells. The latter results further support a cell-autonomous mechanism for the proresilient effect of HDAC6 depletion in 5-HT circuits.

To determine whether diverging transcriptional responses to subchronic GR activation in WT and HDAC6^{Pet1Cre} KO brains coincide with differential neurophysiological adaptations of 5-HT neurons, whole-cell recordings of DR 5-HT neurons were conducted under the same DEX treatment regimen. DR brain slices were collected 1 h after the last administration of VEH or DEX, and recordings were conducted either in the absence or presence of bath-applied DEX (100 μM). While acute bath application of DEX to tissues from VEH-treated mice was devoid of electrophysiological effect (data not shown), subchronic DEX treatment fully recapitulated the effects of social defeat on the excitability of 5-HT neurons. Thus, like social defeat (Fig. 6), subchronic DEX inhibited the ability of WT 5-HT neurons to fire action potentials in response to graded current inputs, but was devoid of effect in HDAC6^{Pet1Cre} KOs (Fig. 9*b*; three-way ANOVA, genotype by treatment by input current interaction, $F_{(4,104)} = 3.09$, $p = 0.01$). Together, these results identify repeated GR activation as a likely mechanism promoting the hypoexcitability of 5-HT neurons during social defeat and confirm the critical dependence of this mechanism on HDAC6 activity.

Serotonergic depletion of HDAC6 alters the socioaffective effects of glucocorticoid hormones

Results presented above suggest that HDAC6 depletion modulates neuroadaptive responses of 5-HT circuits under chronic stress, in part by blocking some of the slow "genomic" actions of adrenal steroids released during repeated social confrontations. However, adrenal steroids, such as Cort and cortisol, also exert rapid behavioral and cognitive effects in animals and humans, detectable a few minutes after exogenous hormone administra-

tion and thus presumably independent of gene transcription or *de novo* protein synthesis (Gasser et al., 2009). Because certain rapid "nongenomic" effects of steroid hormones have been attributed to the signaling activity of certain components of the chaperone complex, released from their interaction with Hsp90 upon hormone stimulation (Han et al., 2009; Groeneweg et al., 2012), we asked whether the rapid socioaffective effects of exogenous glucocorticoids also differ between WT and HDAC6 KO mice.

We first examined the ability of acute exogenous Cort to alter the expression of the resilient or vulnerable behavioral phenotype in a social avoidance test. Mice were exposed to repeated social defeat and were subsequently tested twice for social avoidance, 1 week apart with or without Cort administered in a counterbalanced order. Results from the tests conducted under vehicle conditions were used to stratify individual mice as resilient or vulnerable. When administered as a single injection 20 min before the social interaction task, a low dose of Cort (0.5 mg/kg, i.p) did not influence social approach in control mice (interaction ratio: WT VEH, 146.5 ± 18.2; WT Cort, 160.3 ± 14.5; KO VEH, 142.3 ± 11.3; KO Cort, 139.5 ± 16.6; $n = 13–22$/group) and was devoid of effect on the expression of social avoidance in vulnerable mice, in both genotypes (Fig. 10*a*). However, the same single Cort injection was sufficient to trigger the expression of social avoidance in otherwise nonavoiding defeat-exposed WT mice, thus switching their behavioral profile from defeat-resilient (average interaction ratio, 138.50 ± 10.80) to defeat-vulnerable (average interaction ratio, 85.24 ± 8.51; $F_{(1,14)} = 10.05$; $p = 0.007$). These results indicate that experience-dependent expression of social avoidance in WT mice is facilitated by an acute surge in adrenal steroids and GR activation at the time of testing. In contrast, acute corticosterone administration was devoid of effect in resilient HDAC6^{Pet1Cre} KO mice. Thus, the rapid facilitating effect of adrenal steroids on social avoidance after defeat, which likely reflects nongenomic action of glucocorticoids, also requires intact HDAC6 in 5-HT neurons. Modulation of the rapid behavioral effect of Cort by HDAC6 was not restricted to mice exposed to social defeat, as differential behavioral responses to Cort were also detected in a cohort of naive WT and HDAC6^{Pet1Cre} KO mice examined in two anxiety tasks, the EPM and OF. In these tests, acute Cort induced robust anxiogenic responses in WT mice (i.e., decreased time spent in the center of the OF and open arms of the EPM), while it produced no significant effects, or anxiolytic-like responses in HDAC6^{Pet1Cre} KO mice (Fig. 10*b*; OF test, genotype by treatment interaction, $F_{(1,65)} = 19.8$, $p = 0.00004$; Fisher's PLSD, $p = 0.001$ vs vehicle in WT and $p = 0.05$ vs vehicle in KO; EPM test, genotype by treatment interaction, $F_{(1,34)} = 14.7$, $p = 0.0005$; Fisher's PLSD, $p = 0.001$ vs vehicle in WT).

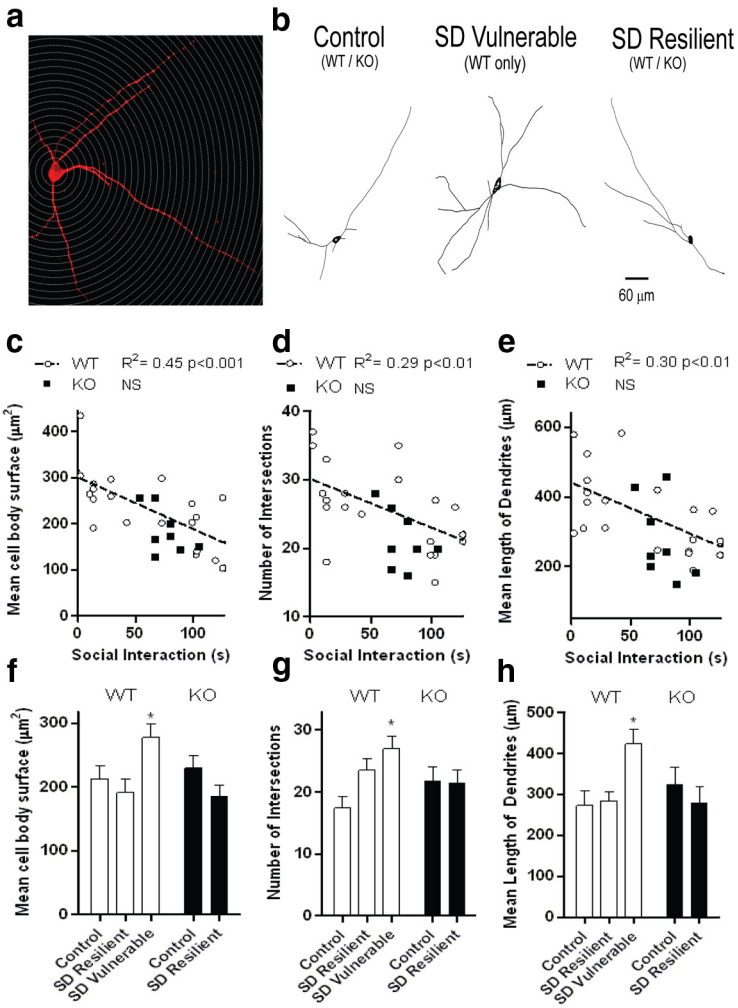

Figure 7. Defeat-induced hypertrophy of serotonin neurons is prevented by HDAC6 depletion. ***a***, Confocal scans from biocytin-filled cells were used to produce 3D reconstructions of 5-HT neurons. Neurons were submitted to Sholl's analyses where the intersections of the dendritic tree with concentric circles spaced every 20 μm from the cell body were used as quantitative indices of cell complexity. ***b***, Representative Neurolucida drawings illustrate the somatodendritic hypertrophy of 5-HT neurons observed most prominently in individual WT mice that expressed the strongest social avoidance responses after social defeat (vulnerable). ***c–e***, In WT mice exposed to defeat (open circles and dotted line), significant correlations were observed between the time spent in interaction zone (target present) and morphological variables including the cumulative number of Sholl intersections within 140 μm from soma, mean cell body surface, and mean dendrite length. No significant correlations were observed in HDAC6^{Pet1Cre} KO mice (black squares). ***f–h***, WT 5-HT neurons from vulnerable mice had a significantly increased cell body area and dendritic length compared with both control and resilient mice. WT vulnerable mice, unlike resilients, also had a higher number of Sholl intersections than control mice. No significant morphological differences were seen in control and social defeat-exposed mice of HDAC6^{Pet1Cre} genotype (*post hoc* comparisons, $^*p < 0.05$ vs control; $n = 8–10$ per condition, except $n = 1$ for KO vulnerable that was excluded from group comparisons). Error bars indicate SEM.

Because Pet1 expression was recently reported in the pancreas (Ohta et al., 2011) where HDAC6 could also regulate GR signaling, it is possible that Pet1-driven recombination may influence glucose homeostasis. We verified that differential behavioral responses to acute corticosteroids in WT and HDAC6^{Pet1Cre} KO mice do not reflect differential plasma glucose regulation under baseline conditions or after corticosterone administration. Despite a significant enhancement of plasma glucose with Cort (WT baseline, 110 ± 6.5 mg/dl; WT Cort, 161.2 ± 17.6 mg/dl; main effect of Cort, $F_{(1,16)} = 19.5$, $p < 0.001$; Fisher's PLSD, $p < 0.01$), there was no significant effect of genotype or interaction between

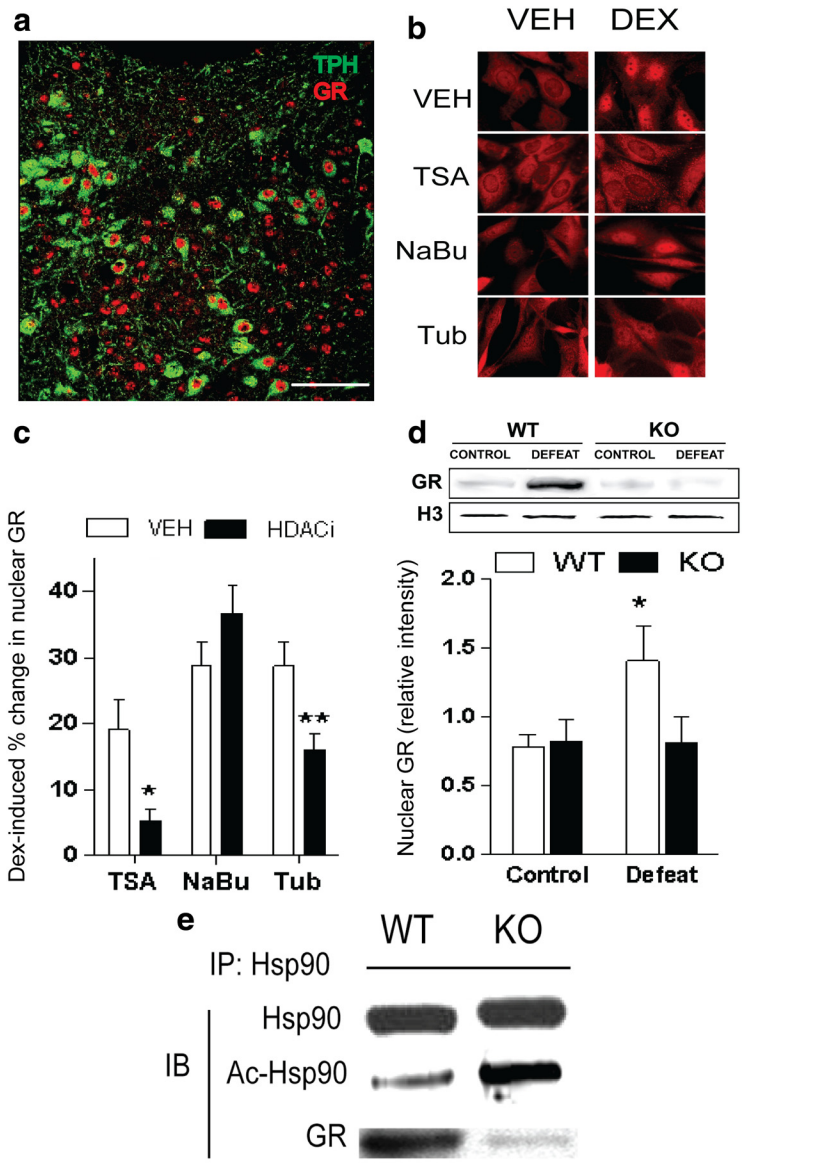

Figure 8. Pharmacological and genetic inactivation of HDAC6 impairs GR chaperoning and blunts hormone- and stress-induced GR nuclear translocation. ***a***, Confocal scan of the DR (40×) shows dual immunostaining for GR (red) and the 5-HTergic marker tryptophan hydroxylase (TPH, green). GR is expressed by most TPH $^{+}$ cells but also by some TPH $^{-}$ cells. ***b***, ***c***, Effect of HDAC6 on GR responses to hormonal stimulation in the RN46A immortalized raphe precursor cell line. ***b***, In the absence of HDAC inhibitor pretreatment (VEH), DEX (1 μM) produces a shift from predominantly cytoplasmic GR immunostaining to a predominantly nuclear signal. Pretreatment with TSA (5 μM) and tubacin (Tub, 10 μM), two inhibitors with nanomolar affinity for HDAC6 prevented DEX-induced nuclear localization of GR, while the selective class I HDAC inhibitor NaBu (1 mM) was devoid of effect. ***c***, Corresponding quantitative measures of DEX-induced changes in GR signal normalized to respective vehicle conditions (*$p < 0.05$, **$p < 0.01$, compared with VEH; $n = 22–69$ cells per condition). ***d***, Thirty minutes following social defeat, the amount of nuclear GR increases significantly in the DR of WT mice, while pan-neuronal HDAC6 KO mice show no increase in nuclear GR in the DR at this time point. Representative bands are shown for each group (*$p < 0.05$, compared with WT control; $n = 4–7$ samples/group). ***e***, Lysates from HDAC6 KO tissues were immunoprecipitated for total Hsp90 and blotted for acetylated Hsp90 (AcHsp90, K294), GR, or total Hsp90. While total levels of Hsp90 were not different between WT and KO mice, Hsp90 acetylation was increased upon neuronal depletion of HDAC6. Under these conditions, the association between Hsp90 and GR was dramatically diminished. Error bars indicate SEM.

Cort and genotype on glucose levels (KO baseline, 113.8 ± 7.8 mg/dl; KO Cort, 160.8 ± 9.0 mg/dl). Thus, despite a lack of significant baseline phenotypic differences between WT and HDAC6^{Pet1Cre} KO mice in socioaffective behaviors, an acute rise in adrenal steroid hormones unmasks such differences in a context- and experience-dependent manner, through a 5-HT- and HDAC6-mediated mechanism.

Discussion

This study identifies HDAC6 as a novel key regulator of stress resilience. Our results indicate that the socioaffective sequelae of social defeat, a murine model of traumatic stress, are mediated in least in part by glucocorticoid hormones and GR activation in serotonin pathways. We provide evidence that these GR-mediated neurobehavioral consequences of social defeat are critically gated through reversible acetylation of Hsp90, a key component of the GR chaperone complex. We present pharmacological and genetic evidence, summarized in Figure 11, indicating that the cytoplasmic lysine deacetylase HDAC6 controls Hsp90 acetylation in the brain and thereby modulates Hsp90–GR protein–protein interactions with inhibitory impact on GR downstream signaling and stress sensitivity

Lack of major contribution of HDAC6 to the development of serotonin neurons

Our neuroanatomical mapping studies identify ascending raphe serotonergic neurons as the densest cell population expressing HDAC6 in the mouse brain. We find that a loss of function of HDAC6 in raphe neurons promotes α-tubulin K40 hyperacetylation without concomitant changes in bulk histone H3 and H4 acetylation. These results extend to the brain a number of previous observations indicative of a limited contribution of HDAC6 to chromatin regulation (Hubbert et al., 2002). Despite its enrichment in 5-HT neurons, HDAC6 did not appear to play a critical role in the embryologic development of this neuronal population. The Pet1-Cre transgenic line used in this study starts driving Cre-recombinase expression on E12.5. Thus, HDAC6 depletion presumably leads to a loss of deacetylase function that encompasses the entire period of the differentiation of 5-HT neurons. Yet, we observed no major change in the number, morphology, and distribution of the somas and axon terminals of 5-HT neurons under baseline conditions. This result was somewhat unexpected as recent neuronal tissue culture studies have shown that loss of function of HDAC6 and resulting protein hyperacetylation during early stages of axonal growth have detrimental effects on axonal elongation and polarization, as well as on the regulation of dendritic branching (Kim et al., 2009; Tapia et al., 2010). Furthermore, a mutation recently identified in human HDAC6 has been linked with a rare skeletal disorder associated with mental retardation (Simon et al., 2010). It should be noted, however, that the latter mutation produces a gain

and not a loss of function of HDAC6. It is possible that depletion of HDAC6 occurring at an earlier stage of the development of 5-HT neural precursors would produce more severe consequences than the current manipulation. However, this view is not supported by earlier studies in constitutive HDAC6 KOs that demonstrated a lack of gross brain cytoarchitectural abnormalities (Zhang et al., 2008). While no morphological abnormalities were found here in neurons of unstressed HDAC6 KO mice, we nonetheless detected certain electrophysiological alterations in naive mice, the most significant of which was a 50% decrease in the input resistance of DR 5-HT neurons. This electrophysiological consequence of HDAC6 KO, which may reflect changes in the synaptic input or expression or distribution of ion channels in 5-HT neurons, was not associated, under whole-cell recording conditions, with changes in the capacity of 5-HT neurons to fire action potentials.

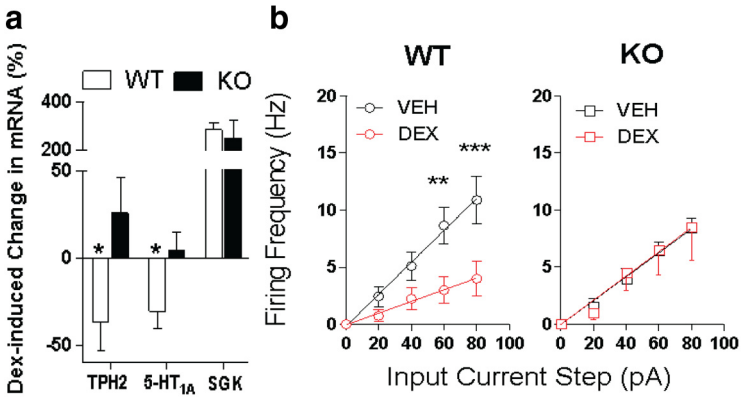

Figure 9. HDAC6 depletion blunts the transcriptional and electrophysiological effects of GR activation in 5-HT neurons. ***a***, In WT mice, subchronic GR activation with DEX (1 mg/kg daily for 4 d) leads to a significant reduction in the expression of TPH2 and 5-HT_{1A}, two transcriptional targets of GR in the serotonin system. The repressive effect of GR stimulation on these two target genes was absent in HDAC6 ^{Pet1Cre} KO mice that lack HDAC6 exclusively in 5-HT neurons. Note, in contrast, the lack of genotype dependence in the stimulatory effect of DEX on expression the canonical GR target gene SGK that is ubiquitously expressed by 5-HT and non-5-HT neurons (*post hoc* comparisons, $*p < 0.05$, compared with WT; $n = 5–9$ per condition). ***b***, Subchronic dexamethasone (1 mg/kg daily for 4 d plus 100 μM bath application) mimics the differential effects of social defeat on the excitability of 5-HT neurons in WT and HDAC6 ^{Pet1Cre} KO mice. DEX reduces the firing frequency of 5-HT neurons in WT mice in a social defeat-like manner (Fig. 6) but is devoid of effect in HDAC6 ^{Pet1Cre} KO mice (*post hoc*, $*p < 0.05$, $**p < 0.01$, $***p < 0.001$, compared with VEH; $n = 8–9$ cells per condition). Error bars indicate SEM.

Novel role of HDAC6 in resilience and stress-induced neuroplasticity of serotonin neurons

In contrast to the lack of behavioral phenotype observed in HDAC6 KOs under baseline conditions, our behavioral results revealed a consistent antidepressant-like influence of serotonergic HDAC6 depletion in mice exposed to severe inescapable stressors. This effect coincided with the prevention of morphological and electrophysiological changes induced in 5-HT neurons by chronic exposure to inescapable social threats. More specifically, our findings indicate that HDAC6-depleted 5-HT neurons were protected from the hypoexcitability and somatodendritic hypertrophy observed in WT mice after repeated social defeat. Although hypoexcitability of 5-HT neurons is a consequence of chronic stress that has been reported previously (Bambico et al., 2009), this is to our knowledge the first demonstration of stress-induced morphological alterations in 5-HT neurons. It is currently unclear whether these electrophysiological and morphological consequences of social defeat in 5-HT neurons are interdependent and whether they are causally linked to the behavioral sequelae of social defeat. However, our results indicated that increased soma size as well as length and complexity of the dendrites of 5-HT neurons after social defeat are strongly correlated with the occurrence of social avoidance. This is in contrast to the defeat-induced hypoexcitability of 5-HT neurons, which was observed in all social defeat-exposed WT mice, independently of their degree of behavioral resilience. The latter electrophysiological change, which was fully recapitulated by subchronic dexamethasone administration, could contribute to reducing functional output of 5-HT neurons in raphe circuits and projection areas in defeated animals. It will be of interest in future studies to determine the impact that stress-induced neuroplastic changes in raphe circuits have at the systems level and to dissect whether their morphological and physiological components are each sufficient or necessary for the expression of social avoidance. Our observation that downregulation of HDAC6 occurs in raphe neurons after social defeat in resilient but not vulnerable mice suggests that changes in HDAC6 may be part of an adaptive mechanism allowing maintenance raphe circuits homeostasis and promoting the expression of behavioral strategies

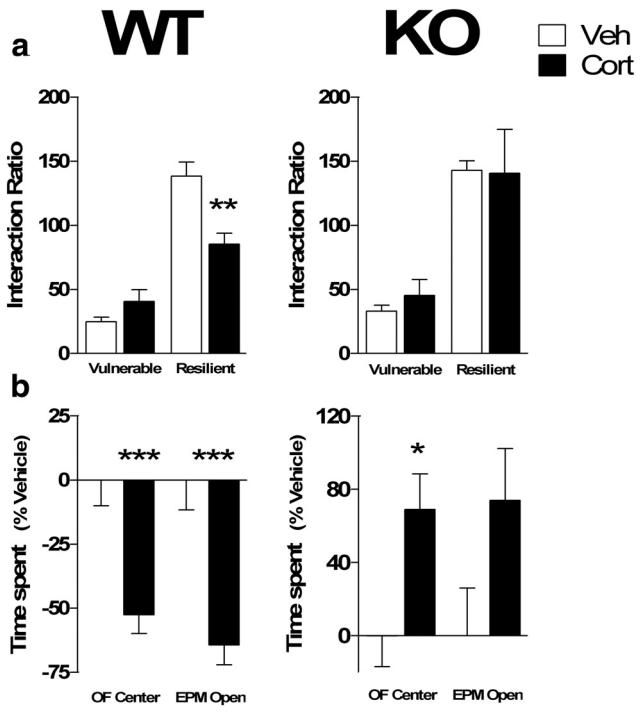

Figure 10. Serotonin-selective depletion of HDAC6 alters socioaffective responses to exogenous corticosterone. ***a***, Depiction of the effect of acute Cort (0.5 mg/kg) or vehicle in the social interaction paradigm. Acute Cort, given 20 min before social avoidance testing, triggered the expression of social avoidance (interaction ratio < 100) in WT social defeat-resilient mice but did not affect social approach toward a CD1 target in control mice or in social defeat-vulnerable mice from both genotypes. This permissive effect of Cort on social avoidance was not seen in resilient HDAC6 ^{Pet1Cre} KO mice (right column; $**p < 0.01$, compared with vehicle). ***b***, Depicts the effect of Cort or vehicle treatment in the OF and the EPM. Cort injection 20 min before testing induced anxiogenic responses in WT mice (i.e., decreased time spent in the center of the OF and open arms of EPM), while it produced no significant effects or induced anxiolytic-like responses (i.e., increased time spent in the center of an open field) in HDAC6 ^{Pet1Cre} KO mice (*post hoc* comparisons, $*p < 0.05$, $***p < 0.001$, compared with vehicle; $n = 13–22$ per condition). Error bars indicate SEM.

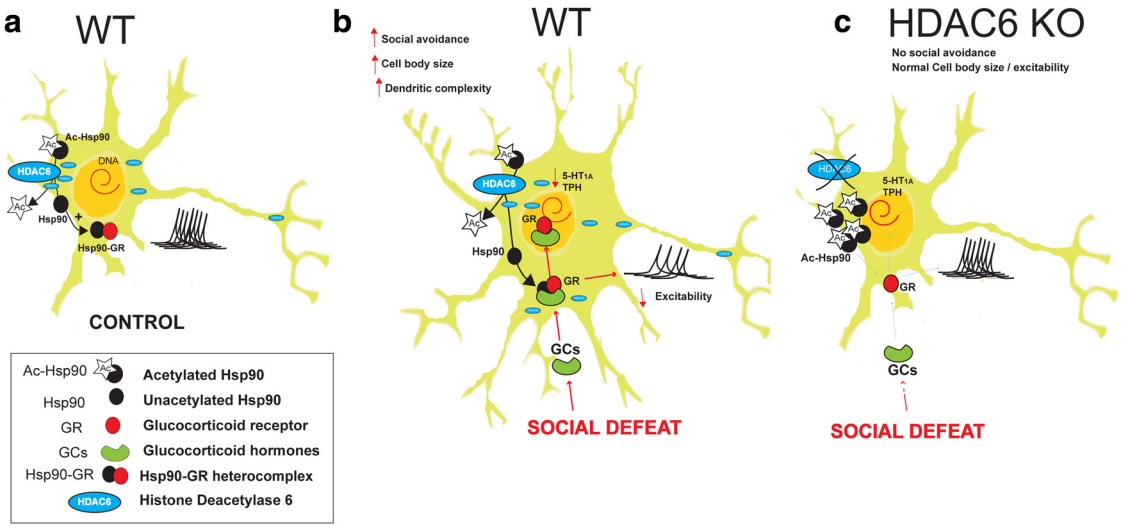

Figure 11. HDAC6 gates GR-mediated neuroplasticity in serotonin neurons with critical impact on affective resilience. This figure depicts a dorsal raphe serotonin neuron expressing HDAC6 and GR and summarizes the hypothesized role of these two proteins in the diverging behavioral phenotype and the differential neuroplastic changes observed in WT and HDAC6 KO mice exposed to severe stress. ***a***, Under physiological conditions, HDAC6 deacetylates Hsp90 and thereby enables the formation of the Hsp90 –GR heterocomplex critical for the folding and maturation of GR into a hormone binding competent receptor. ***b***, Stimulation of GR by glucocorticoid hormones (GCs) released during social defeat induces GR nuclear translocation that leads to a downregulation of multiple serotonergic GR target genes including 5-HT_{1A} and TPH. Social defeat also results in an increase in the soma size and length and complexity of serotonergic neuronal processes, a series of morphological changes that correlate strongly with the individual expression of social avoidance. Social defeat also renders serotonin neurons hypoexcitable, an electrophysiological change that can, like social avoidance, be recapitulated by exogeneous administration of GCs. ***c***, Genetic depletion of HDAC6 results in the expression of a resilient behavioral phenotype associated with the hyperacetylation of Hsp90, reduced interactions of HSP90 and GR, and a loss of GR translocation during social defeat. These changes are thought to reflect, in part, the misfolding and decreased affinity of GR for GCs (Murphy et al., 2005). Coincidently, 5-HT neurons of HDAC6 KO mice, in contrast to those of WT mice, maintain normal excitability and do not develop somatodendritic hypertrophy upon exposure to social defeat.

that are adaptative in the context of this social defeat paradigm, such as risk assessment behaviors. The finding that imipramine (this study) but also antidepressants from other chemical classes (Chen et al., 2010; Mao et al., 2011) downregulate HDAC6 expression and function suggest that HDAC6-dependent signaling cascades may constitute a downstream target shared by several antidepressant compounds. It will thus be of interest to determine, in future studies, how newly discovered HDAC inhibitors with improved selectivity for HDAC6 (Butler et al., 2010) influence the function of serotonergic circuits and behavior in stress-exposed animals.

Blunted GR signaling in serotonin neurons mediates the resilient phenotype of HDAC6 KO mice

The behavioral and neuroendocrine impact of GR activation is well characterized in key forebrain circuits involved in the feedback regulation of the HPA axis. In these areas, increasing GR signaling has typically been associated with facilitating the termination of stress and promoting antidepressant-like responses (Anacker et al., 2011). However, less is known about the role of GR in brainstem and midbrain areas, such as the raphe nuclei, where this receptor is also abundantly expressed (Chaouloff, 2000; Wylie et al., 2010). To our knowledge, no data are available currently regarding the effects of serotonin-specific ablation of GR in the raphe nuclei. Based on earlier pharmacological studies, brainstem GR is thought to mediate rapid stress-like behavioral, autonomic, and electrophysiological responses (Gasser et al., 2009). Two lines of evidence in the present study suggest that the pulsatile activation of GR and resulting downstream effects in raphe neurons may be critical for the induction and/or expression of social avoidance after social defeat. First, in line with previous studies, we found that GR is highly expressed by raphe serotonin neurons (Wylie et al., 2010) and that social defeat stimulates GR signaling and induces translocation of GR locally in the DR. Second, we found that this effect is fully blocked upon selective inactivation of HDAC6 in 5-HT neurons, in conjunction with a loss of the ability of GR agonists to precipitate the expression of social avoidance, to induce a hypoexcitability of 5-HT neurons and to promote transcriptional repression of serotonergic target genes (Fig. 11). Finally, we found that serotonergic depletion of HDAC6 shifts the typically anxiogenic activity of acute corticosterone in EPM and OF toward an anxiolytic-like activity. Because HDAC6 inhibition leads to a 100- to 1000-fold reduction in hormone binding at GR (Murphy et al., 2005), we interpret the paradoxical behavioral response in $HDAC6^{Pet1Cre}$ KO mice, which resembles the effects of GR antagonists, as a component of the corticosterone response typically overshadowed in presence of fully functional raphe GR signaling. This unmasked component could reflect aspects of mineralocorticoid- or membrane-mediated signaling by glucocorticoids that are independent of the role of HDAC6 in 5-HT circuits. Our pharmacological data are in line with previous results in rodents that support the involvement of both rapid nongenomic and slower transcription-dependent effects of corticosteroids in the modulation of socioaffective behaviors (Gasser et al., 2009), which both appear to be dependent on HDAC6. However, in line with recent report in global HDAC6 knock-out, the activity of HDAC6 as regulator of GR response in the brain appears relatively circumscribed to certain circuits and does not appear to have a broad impact on HPA axis regulation (Winkler et al., 2012).

HDAC6-mediated modulation of GR chaperone function as a novel strategy for proresilience interventions

Our experiments examining aspects of GR signaling in HDAC6-depleted 5-HT neurons support a link between proresilient effects of HDAC6 depletion and regulation of the GR chaperone complex. HDAC6 has previously been shown to regulate GR chaperoning via reversible acetylation of Hsp90, a key compo-

nent of the GR chaperone complex (Aoyagi and Archer, 2005; Kovacs et al., 2005; Murphy et al., 2005; Zhang et al., 2008). While this role of HDAC6 in modulating the dynamic association of Hsp90 and GR has been well established in non-neuronal tissues, it had never been directly examined in the CNS *in vivo*. Our results indicate that this role fully extends to the brain, with a dramatic impact on the neurobehavioral effects of glucocorticoids. Previous Hsp90 mutagenesis studies have shown that mutations that mimic lysine hyperacetylation at certain residues disrupt the ability of Hsp90 to interact with steroid receptor clients and certain GR cochaperones, such as the FKBP51/52 immunophilins (Scroggins et al., 2007) that have previously been involved in stress-related disorders (Binder, 2009). Functionally, Hsp90 hyperacetylation has been shown to reduce the hormone response of GR by 100- to 1000-fold (Murphy et al., 2005). This goes along with the dramatically reduced GR responses observed in most of our assays after HDAC6 depletion. Of note, it is possible that Hsp90 hyperacetylation also affected the signaling of other steroid receptors in the DR with known influence on affective behaviors, such as the androgen and estrogen receptors (Fiskus et al., 2007; Ai et al., 2009). Experiments currently ongoing in our laboratory are testing these possibilities and evaluating the capability of a nonacetylatable Hsp90 point mutant, overexpressed in DR, to rescue GR responsivity and stress vulnerability in HDAC6 KOs. Because genetic variations that affect the stoichiometry of GR chaperone complex have been previously associated with increased risk to develop stress-related affective disorders and individual variability in therapeutic responses to antidepressants (Binder et al., 2004; Maeng et al., 2008; Binder, 2009; Hunsberger et al., 2009), it is tempting to speculate that pharmacological modulation of GR chaperone dynamics using HDAC6 inhibitors may be of therapeutic value for the treatment of stress-related disorders. In conclusion, our results identify HDAC6 as a novel target for proresilience and antidepressant interventions through focal inhibition of GR signaling in serotonin neurons and uncover an alternate mechanism by which pan-HDAC inhibitors may regulate stress-related behaviors independently of their influence on histones.

Note added in proof. While this manuscript was in press, two papers were published reporting converging roles of HDAC6 in glucocorticoid signaling and the regulation emotional responses in rodents. Fukada et al. (2012) reported a cellular distribution of HDAC6 consistent with the one described here and showed that global loss of HDAC6 leads to an antidepressant-like phenotype. Lee et al. (2012) showed that inhibition of HDAC6 in the rat medial prefrontal cortex inhibits GR signaling in layer V pyramidal cells and blocks synaptic effects of acute stress.

References

Ai J, Wang Y, Dar JA, Liu J, Liu L, Nelson JB, Wang Z (2009) HDAC6 regulates androgen receptor hypersensitivity and nuclear localization via modulating Hsp90 acetylation in castration-resistant prostate cancer. Mol Endocrinol 23:1963–1972.

Akhtar MW, Raingo J, Nelson ED, Montgomery RL, Olson EN, Kavalali ET, Monteggia LM (2009) Histone deacetylases 1 and 2 form a developmental switch that controls excitatory synapse maturation and function. J Neurosci 29:8288–8297.

Albert PR, Lemonde S (2004) 5-HT1A receptors, gene repression, and depression: guilt by association. Neuroscientist 10:575–593.

Allen Institute for Brain Science, Royall JJ, Ng LL, Morris JA (2008) Dorsal nucleus raphé (DR). Allen Brain Atlas annotation report. Nature Precedings. Advance online publication. Retrieved February 21, 2012. doi:10.1038/npre.2008.2054.1.

Anacker C, Zunszain PA, Carvalho LA, Pariante CM (2011) The glucocorticoid receptor: pivot of depression and of antidepressant treatment? Psychoneuroendocrinology 36:415–425.

Aoyagi S, Archer TK (2005) Modulating molecular chaperone Hsp90 functions through reversible acetylation. Trends Cell Biol 15:565–567.

Azmitia EC, Liao B (1994) Dexamethasone reverses adrenalectomy-induced neuronal de-differentiation in midbrain raphe-hippocampus axis. Ann N Y Acad Sci 746:180–193; discussion 193–194, 221–222.

Azmitia EC, Liao B, Chen YS (1993) Increase of tryptophan hydroxylase enzyme protein by dexamethasone in adrenalectomized rat midbrain. J Neurosci 13:5041–5055.

Bali P, Pranpat M, Bradner J, Balasis M, Fiskus W, Guo F, Rocha K, Kumaraswamy S, Boyapalle S, Atadja P, Seto E, Bhalla K (2005) Inhibition of histone deacetylase 6 acetylates and disrupts the chaperone function of heat shock protein 90: a novel basis for antileukemia activity of histone deacetylase inhibitors. J Biol Chem 280:26729–26734.

Bambico FR, Nguyen NT, Gobbi G (2009) Decline in serotonergic firing activity and desensitization of 5-HT1A autoreceptors after chronic unpredictable stress. Eur Neuropsychopharmacol 19:215–228.

Beck SG, Pan YZ, Akanwa AC, Kirby LG (2004) Median and dorsal raphe neurons are not electrophysiologically identical. J Neurophysiol 91:994–1005.

Berton O, McClung CA, Dileone RJ, Krishnan V, Renthal W, Russo SJ, Graham D, Tsankova NM, Bolanos CA, Rios M, Monteggia LM, Self DW, Nestler EJ (2006) Essential role of BDNF in the mesolimbic dopamine pathway in social defeat stress. Science 311:864–868.

Berton O, Covington HE 3rd, Ebner K, Tsankova NM, Carle TL, Ulery P, Bhonsle A, Barrot M, Krishnan V, Singewald GM, Singewald N, Birnbaum S, Neve RL, Nestler EJ (2007) Induction of deltaFosB in the periaqueductal gray by stress promotes active coping responses. Neuron 55:289–300.

Bethea CL, Lu NZ, Reddy A, Shlaes T, Streicher JM, Whittemore SR (2003) Characterization of reproductive steroid receptors and response to estrogen in a rat serotonergic cell line. J Neurosci Methods 127:31–41.

Binder EB (2009) The role of FKBP5, a co-chaperone of the glucocorticoid receptor in the pathogenesis and therapy of affective and anxiety disorders. Psychoneuroendocrinology 34 [Suppl 1]:S186–S195.

Binder EB, Salyakina D, Lichtner P, Wochnik GM, Ising M, Pütz B, Papiol S, Seaman S, Lucae S, Kohli MA, Nickel T, Künzel HE, Fuchs B, Majer M, Pfennig A, Kern N, Brunner J, Modell S, Baghai T, Deiml T, et al. (2004) Polymorphisms in FKBP5 are associated with increased recurrence of depressive episodes and rapid response to antidepressant treatment. Nat Genet 36:1319–1325.

Bobrowska A, Paganetti P, Matthias P, Bates GP (2011) Hdac6 knock-out increases tubulin acetylation but does not modify disease progression in the R6/2 mouse model of Huntington's disease. PLoS One 6:e20696.

Bradner JE, West N, Grachan ML, Greenberg EF, Haggarty SJ, Warnow T, Mazitschek R (2010) Chemical phylogenetics of histone deacetylases. Nat Chem Biol 6:238–243.

Braz JM, Enquist LW, Basbaum AI (2009) Inputs to serotonergic neurons revealed by conditional viral transneuronal tracing. J Comp Neurol 514:145–160.

Butler KV, Kalin J, Brochier C, Vistoli G, Langley B, Kozikowski AP (2010) Rational design and simple chemistry yield a superior, neuroprotective HDAC6 inhibitor, tubastatin A. J Am Chem Soc 132:10842–10846.

Calizo LH, Akanwa A, Ma X, Pan YZ, Lemos JC, Craige C, Heemstra LA, Beck SG (2011) Raphe serotonin neurons are not homogenous: electrophysiological, morphological and neurochemical evidence. Neuropharmacology 61:524–543.

Chaouloff F (2000) Serotonin, stress and corticoids. J Psychopharmacol 14:139–151.

Charuvastra A, Cloitre M (2008) Social bonds and posttraumatic stress disorder. Annu Rev Psychol 59:301–328.

Chen S, Owens GC, Makarenkova H, Edelman DB (2010) HDAC6 regulates mitochondrial transport in hippocampal neurons. PloS One 5:e10848.

Choudhary C, Kumar C, Gnad F, Nielsen ML, Rehman M, Walther TC, Olsen JV, Mann M (2009) Lysine acetylation targets protein complexes and co-regulates major cellular functions. Science 325:834–840.

Clark JA, Flick RB, Pai LY, Szalayova I, Key S, Conley RK, Deutch AY, Hutson PH, Mezey E (2008) Glucocorticoid modulation of tryptophan hydroxylase-2 protein in raphe nuclei and 5-hydroxytryptophan concentrations in frontal cortex of C57/Bl6 mice. Mol Psychiatry 13:498–506.

Covington HE 3rd, Maze I, LaPlant QC, Vialou VF, Ohnishi YN, Berton O, Fass DM, Renthal W, Rush AJ 3rd, Wu EY, Ghose S, Krishnan V, Russo SJ, Tamminga C, Haggarty SJ, Nestler EJ (2009) Antidepressant actions of histone deacetylase inhibitors. J Neurosci 29:11451–11460.

Crawford LK, Craige CP, Beck SG (2010) Increased intrinsic excitability of lateral wing serotonin neurons of the dorsal raphe: a mechanism for selective activation in stress circuits. J Neurophysiol 103:2652–2663.

Crowley JJ, Jones MD, O'Leary OF, Lucki I (2004) Automated tests for measuring the effects of antidepressants in mice. Pharmacol Biochem Behav 78:269–274.

Cryan JF, Markou A, Lucki I (2002) Assessing antidepressant activity in rodents: recent developments and future needs. Trends Pharmacol Sci 23:238–245.

Dayan P, Huys QJ (2009) Serotonin in affective control. Annu Rev Neurosci 32:95–126.

Fiskus W, Ren Y, Mohapatra A, Bali P, Mandawat A, Rao R, Herger B, Yang Y, Atadja P, Wu J, Bhalla K (2007) Hydroxamic acid analogue histone deacetylase inhibitors attenuate estrogen receptor-alpha levels and transcriptional activity: a result of hyperacetylation and inhibition of chaperone function of heat shock protein 90. Clin Cancer Res 13:4882–4890.

Fukada M, Hanai A, Nakayama A, Suzuki T, Miyata N, Rodriguiz RM, Wetsel WC, Yao TP, Kawaguchi Y (2012) Loss of deacetylation activity of hdac6 affects emotional behavior in mice. PloS One 7:e30924.

Gao YS, Hubbert CC, Lu J, Lee YS, Lee JY, Yao TP (2007) Histone deacetylase 6 regulates growth factor-induced actin remodeling and endocytosis. Mol Cell Biol 27:8637–8647.

Gasser PJ, Lowry CA, Orchinik M (2009) Rapid corticosteroid actions on behavior: mechanisms and implications. In: Hormones, brain and behavior (Pfaff DW, Arnold AP, Fahrbach SE, Etgen AM, Rubin RT, eds), pp 1365–1387. San Diego: Academic.

Golden SA, Covington HE 3rd, Berton O, Russo SJ (2011) A standardized protocol for repeated social defeat stress in mice. Nat Protoc 6:1183–1191.

Groeneweg FL, Karst H, de Kloet ER, Joëls M (2012) Mineralocorticoid and glucocorticoid receptors at the neuronal membrane, regulators of nongenomic corticosteroid signalling. Mol Cell Endocrinol 350:299–309.

Haggarty SJ, Tsai LH (2011) Probing the role of HDACs and mechanisms of chromatin-mediated neuroplasticity. Neurobiol Learn Mem 96:41–52.

Haggarty SJ, Koeller KM, Wong JC, Grozinger CM, Schreiber SL (2003) Domain-selective small-molecule inhibitor of histone deacetylase 6 (HDAC6)-mediated tubulin deacetylation. Proc Natl Acad Sci U S A 100:4389–4394.

Han G, Ma H, Chintala R, Fulton DJ, Barman SA, White RE (2009) Essential role of the 90-kilodalton heat shock protein in mediating nongenomic estrogen signaling in coronary artery smooth muscle. J Pharmacol Exp Ther 329:850–855.

Hobara T, Uchida S, Otsuki K, Matsubara T, Funato H, Matsuo K, Suetsugi M, Watanabe Y (2010) Altered gene expression of histone deacetylases in mood disorder patients. J Psychiat Res 44:263–270.

Hubbert C, Guardiola A, Shao R, Kawaguchi Y, Ito A, Nixon A, Yoshida M, Wang XF, Yao TP (2002) HDAC6 is a microtubule-associated deacetylase. Nature 417:455–458.

Huhman KL (2006) Social conflict models: can they inform us about human psychopathology? Horm Behav 50:640–646.

Hunsberger JG, Austin DR, Chen G, Manji HK (2009) Cellular mechanisms underlying affective resiliency: the role of glucocorticoid receptor- and mitochondrially-mediated plasticity. Brain Res 1293:76–84.

Kekatpure VD, Dannenberg AJ, Subbaramaiah K (2009) HDAC6 modulates Hsp90 chaperone activity and regulates activation of aryl hydrocarbon receptor signaling. J Biol Chem 284:7436–7445.

Kim AH, Puram SV, Bilimoria PM, Ikeuchi Y, Keough S, Wong M, Rowitch D, Bonni A (2009) A centrosomal Cdc20-APC pathway controls dendrite morphogenesis in postmitotic neurons. Cell 136:322–336.

Kiyasova V, Fernandez SP, Laine J, Stankovski L, Muzerelle A, Doly S, Gaspar P (2011) A genetically defined morphologically and functionally unique subset of 5-HT neurons in the mouse raphe nuclei. J Neurosci 31:2756–2768.

Kovacs JJ, Murphy PJ, Gaillard S, Zhao X, Wu JT, Nicchitta CV, Yoshida M, Toft DO, Pratt WB, Yao TP (2005) HDAC6 regulates Hsp90 acetylation and chaperone-dependent activation of glucocorticoid receptor. Mol Cell 18:601–607.

Krishnan V, Han MH, Graham DL, Berton O, Renthal W, Russo SJ, Laplant Q, Graham A, Lutter M, Lagace DC, Ghose S, Reister R, Tannous P, Green TA, Neve RL, Chakravarty S, Kumar A, Eisch AJ, Self DW, Lee FS, et al. (2007) Molecular adaptations underlying susceptibility and resistance to social defeat in brain reward regions. Cell 131:391–404.

Kudryavtseva NN, Bakshtanovskaya IV, Koryakina LA (1991) Social model of depression in mice of C57BL/6J strain. Pharmacol Biochem Behav 38:315–320.

Lee JB, Wei J, Liu W, Cheng J, Feng J, Yan Z (2012) Histone deacetylase 6 gates the synaptic action of acute stress in prefrontal cortex. J Physiol. Advance online publication. doi:10.1113/jphysiol.2011.224907.

Lemos JC, Pan YZ, Ma X, Lamy C, Akanwa AC, Beck SG (2006) Selective 5-HT receptor inhibition of glutamatergic and GABAergic synaptic activity in the rat dorsal and median raphe. Eur J Neurosci 24:3415–3430.

Maeng S, Hunsberger JG, Pearson B, Yuan P, Wang Y, Wei Y, McCammon J, Schloesser RJ, Zhou R, Du J, Chen G, McEwen B, Reed JC, Manji HK (2008) BAG1 plays a critical role in regulating recovery from both manic-like and depression-like behavioral impairments. Proc Natl Acad Sci U S A 105:8766–8771.

Mao X, Hou T, Cao B, Wang W, Li Z, Chen S, Fei M, Hurren R, Gronda M, Wu D, Trudel S, Schimmer AD (2011) The tricyclic antidepressant amitriptyline inhibits D-cyclin transactivation and induces myeloma cell apoptosis by inhibiting histone deacetylases: in vitro and in silico evidence. Mol Pharmacol 79:672–680.

Matsuyama A, Shimazu T, Sumida Y, Saito A, Yoshimatsu Y, Seigneurin-Berny D, Osada H, Komatsu Y, Nishino N, Khochbin S, Horinouchi S, Yoshida M (2002) In vivo destabilization of dynamic microtubules by HDAC6-mediated deacetylation. EMBO J 21:6820–6831.

Montgomery RL, Hsieh J, Barbosa AC, Richardson JA, Olson EN (2009) Histone deacetylases 1 and 2 control the progression of neural precursors to neurons during brain development. Proc Natl Acad Sci U S A 106:7876–7881.

Murphy PJ, Morishima Y, Kovacs JJ, Yao TP, Pratt WB (2005) Regulation of the dynamics of hsp90 action on the glucocorticoid receptor by acetylation/deacetylation of the chaperone. J Biol Chem 280:33792–33799.

Ohta Y, Kosaka Y, Kishimoto N, Wang J, Smith SB, Honig G, Kim H, Gasa RM, Neubauer N, Liou A, Tecott LH, Deneris ES, German MS (2011) Convergence of the insulin and serotonin programs in the pancreatic beta-cell. Diabetes 60:3208–3216.

Ou XM, Storring JM, Kushwaha N, Albert PR (2001) Heterodimerization of mineralocorticoid and glucocorticoid receptors at a novel negative response element of the 5-HT1A receptor gene. J Biol Chem 276:14299–14307.

Renthal W, Maze I, Krishnan V, Covington HE 3rd, Xiao G, Kumar A, Russo SJ, Graham A, Tsankova N, Kippin TE, Kerstetter KA, Neve RL, Haggarty SJ, McKinsey TA, Bassel-Duby R, Olson EN, Nestler EJ (2007) Histone deacetylase 5 epigenetically controls behavioral adaptations to chronic emotional stimuli. Neuron 56:517–529.

Sapolsky RM (2005) The influence of social hierarchy on primate health. Science 308:648–652.

Scott MM, Wylie CJ, Lerch JK, Murphy R, Lobur K, Herlitze S, Jiang W, Conlon RA, Strowbridge BW, Deneris ES (2005) A genetic approach to access serotonin neurons for in vivo and in vitro studies. Proc Natl Acad Sci U S A 102:16472–16477.

Scroggins BT, Robzyk K, Wang D, Marcu MG, Tsutsumi S, Beebe K, Cotter RJ, Felts S, Toft D, Karnitz L, Rosen N, Neckers L (2007) An acetylation site in the middle domain of Hsp90 regulates chaperone function. Mol Cell 25:151–159.

Simon D, Laloo B, Barillot M, Barnetche T, Blanchard C, Rooryck C, Marche M, Burgelin I, Coupry I, Chassaing N, Gilbert-Dussardier B, Lacombe D, Grosset C, Arveiler B (2010) A mutation in the 3′-UTR of the HDAC6 gene abolishing the post-transcriptional regulation mediated by hsa-miR-433 is linked to a new form of dominant X-linked chondrodysplasia. Hum Mol Genet 19:2015–2027.

Spange S, Wagner T, Heinzel T, Krämer OH (2009) Acetylation of non-histone proteins modulates cellular signalling at multiple levels. Int J Biochem Cell Biol 41:185–198.

Tapia M, Wandosell F, Garrido JJ (2010) Impaired function of HDAC6 slows down axonal growth and interferes with axon initial segment development. PLoS One 5:e12908.

Tsankova NM, Berton O, Renthal W, Kumar A, Neve RL, Nestler EJ (2006) Sustained hippocampal chromatin regulation in a mouse model of depression and antidepressant action. Nat Neurosci 9:519–525.

Verdel A, Curtet S, Brocard MP, Rousseaux S, Lemercier C, Yoshida M, Khochbin S (2000) Active maintenance of mHDA2/mHDAC6 histone-deacetylase in the cytoplasm. Curr Biol 10:747–749.

White LA, Eaton MJ, Castro MC, Klose KJ, Globus MY, Shaw G, Whittemore SR (1994) Distinct regulatory pathways control neurofilament expression and neurotransmitter synthesis in immortalized serotonergic neurons. J Neurosci 14:6744–6753.

Winkler R, Benz V, Clemenz M, Bloch M, Foryst-Ludwig A, Wardat S, Witte N, Trappiel M, Namsolleck P, Mai K, Spranger J, Matthias G, Roloff T, Truee O, Kappert K, Schupp M, Matthias P, Kintscher U (2012) Histone deacetylase 6 (HDAC6) is an essential modifier of glucocorticoid-induced hepatic gluconeogenesis. Diabetes 61:513–523.

Wylie CJ, Hendricks TJ, Zhang B, Wang L, Lu P, Leahy P, Fox S, Maeno H, Deneris ES (2010) Distinct transcriptomes define rostral and caudal serotonin neurons. J Neurosci 30:670–684.

Yang Y, Rao R, Shen J, Tang Y, Fiskus W, Nechtman J, Atadja P, Bhalla K (2008) Role of acetylation and extracellular location of heat shock protein 90alpha in tumor cell invasion. Cancer Res 68:4833–4842.

Zhang Y, Kwon S, Yamaguchi T, Cubizolles F, Rousseaux S, Kneissel M, Cao C, Li N, Cheng HL, Chua K, Lombard D, Mizeracki A, Matthias G, Alt FW, Khochbin S, Matthias P (2008) Mice lacking histone deacetylase 6 have hyperacetylated tubulin but are viable and develop normally. Mol Cell Biol 28:1688–1701.

Zhao S, Xu W, Jiang W, Yu W, Lin Y, Zhang T, Yao J, Zhou L, Zeng Y, Li H, Li Y, Shi J, An W, Hancock SM, He F, Qin L, Chin J, Yang P, Chen X, Lei Q, et al. (2010) Regulation of cellular metabolism by protein lysine acetylation. Science 327:1000–1004.